Recent Progress on the Applications of Carbonaceous and Metal-Organic Framework Nanomaterials for Supercapacitors

Sheng Qiang Zheng[1,2], Siew Shee Lim[1], Chuan Yi Foo[3,4], Choon Yian Haw[3,4], Wee Siong Chiu[5], Chin Hua Chia[6] and Poi Sim Khiew[2]*

[1]Department of Chemical and Environmental Engineering, Faculty of Engineering, The University of Nottingham Malaysia Campus, Semenyih, Malaysia, [2]Center of Nanotechnology and Advanced Materials, Faculty of Science and Engineering, The University of Nottingham Malaysia Campus, Semenyih, Malaysia, [3]School of Energy and Chemical Engineering, Xiamen University Malaysia, Sepang, Malaysia, [4]College of Chemistry and Chemical Engineering, Xiamen University, Xiamen, China, [5]Low Dimensional Materials Research Center, Department of Physics, Faculty of Science, University of Malaya, Kuala Lumpur, Malaysia, [6]Faculty Science and Technology, School of Applied Physics, University Kebangsaan Malaysia, Bangi, Malaysia

Supercapacitors (SCs) have been widely investigated in the realm of energy resulting from their superior long lifespan and remarkable power density. However, their practical usage is limited because of the high effective resistance and relatively low energy density. Electrode material is crucial for determining the performance of SCs, so the innovation and development of advanced electrode materials is particularly important. Metal-organic frameworks (MOFs) and carbonaceous materials, including MOF-derived carbons and carbon nanotubes (CNTs), are befitting as electrode active materials for SCs on the strength of the unique features of high porosity, tunable structures, and easy formation of composites with other compounds. Hence, great efforts were devoted on the synthesis strategies and structural modifications of electrodes to enhance the performance of SCs. In this review, the recent innovations in the realm of SCs, including the application of pristine and derivatives of MOFs as SC electrode materials, were extensively studied. Furthermore, the functions and electrochemical performance of various MOFs and their derivatives (e.g., MOF-derived carbons) were analyzed accordingly. Lastly, the innovations and application of CNTs as SC electrode active materials are systematically summarized. This review highlights the electrochemical performance of some advanced MOF- and carbon-based materials, and the critical factors for SC electrode active materials to achieve excellent electrochemical performance in the application of energy storage systems.

Keywords: metal-organic frameworks, supercapacitors, MOF-derived carbons, carbon nanotubes, electrochemical performance, applications

INTRODUCTION

With the rapid growth in the world population, and the fast development of science and technology, conventional energy sources (such as fossil fuels) are consumed rapidly, resulting in energy crisis and serious global warming. As a consequence, a lot of policies and laws have been introduced to reduce the emission of carbon dioxide (CO_2), the main contributor to the greenhouse effect. These changes have urged researchers to seek for renewable energy resources. Renewable energies, especially solar,

FIGURE 1 | A schematic showing a structure supercapacitor containing cell cases, current collectors, active materials, separator, and electrolyte.
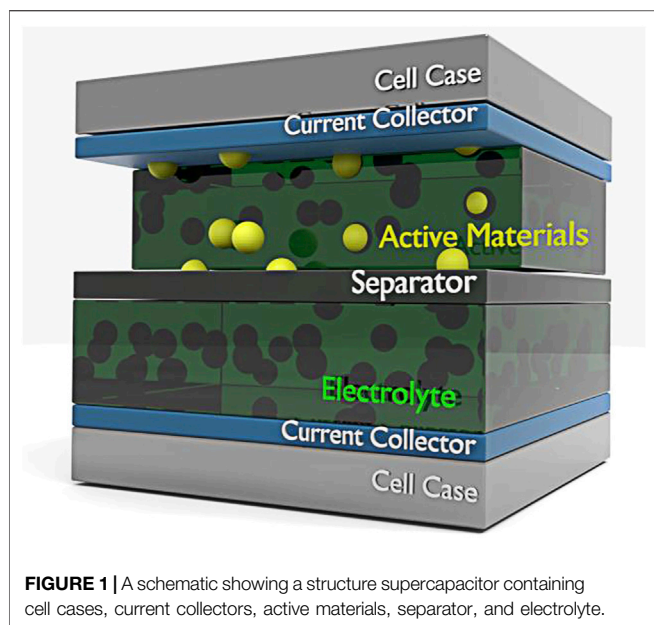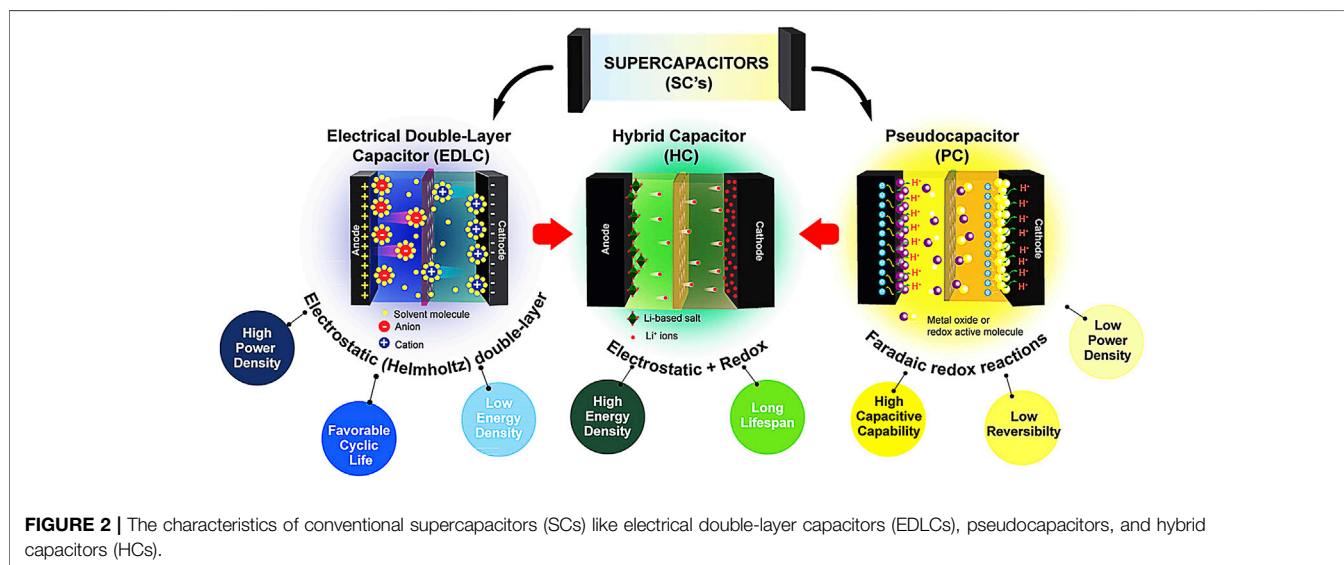
wind, ocean, and geothermal energy, have been developed rapidly in the past two decades. However, the main limitation of these renewable technologies is their inconsistent power output (Xiao et al., 2011). Therefore, this calls for reliable and efficient electrochemical energy storage systems (ESSs) for practical applications. Currently, batteries and SCs are the two main electrochemical energy storage devices. Though batteries with outstanding energy density have dominated the ESSs for decades, they are limited by the inferior rate capability due to the slow redox process and sluggish charge transport (Zheng et al., 2014; Kiani et al., 2015). It is hard to satisfy the energy requirements for sensing devices (Dalstein et al., 2016; Chocarro-Ruiz et al., 2018; Ko et al., 2018; Sezginel et al., 2018), light-emitting diode (Jayananda et al., 2018; Jayananda et al., 2020), digital cameras

(Dalstein et al., 2016), regenerative braking system (Jin et al., 2015; Partridge and Abouelamaimen, 2019), and electrical vehicles (Jin et al., 2015). SCs are emerging as crucial ESSs since they can provide high power density and have long lifecycle as well as the capability of re-energizing in seconds (Kim et al., 2015; Wang et al., 2016; Gautham Prasad et al., 2019). **Figure 1** shows a schematic illustration of the configuration for SCs.

In general, there are three different types of SCs based on interfacial physics and chemistry, namely, electrical double-layer capacitors (EDLCs) (Pavaskar et al., 2018; Gautham Prasad G et al., 2019), pseudocapacitors (Costentin et al., 2017), and hybrid capacitors (HCs) (El-Kady et al., 2015) as illustrated in **Figure 2**. EDLCs store charge through formation of static electrical double layer (known as Helmholtz double-layer) with a high diffusion rate, which enables them to exhibit high power density and excellent cyclability. Nonetheless, they are always characterized with much lower energy densities compared to the other two (Zeng et al., 2019). Unlike EDLCs, the working principle of pseudocapacitors involves reversible Faradic redox reactions, which lead to a higher capacitive capability (Jiang and Liu, 2019). Most of the pseudocapacitors, however, have low cyclic stability and power density (Salunkhe et al., 2017). HCs, formed by combining EDLCs and pseudocapacitors, are found to possess higher energy density and longer lifespan. Commonly, carbon-based active materials like CNTs, activated carbon (AC), graphene, and carbon black with large surface areas are suitable for EDLCs (Rakhi et al., 2012; Jiang et al., 2013; El-Kady et al., 2015; Xia et al., 2017), whereas conducting polymers (Boota and Gogotsi, 2019), transition metal oxides (TMOs) (Zheng et al., 2017), and hydroxides (Salunkhe et al., 2017) are mainly utilized for pseudocapacitors. Thus, it is necessary to explore advanced electrode active materials with high accessible surface areas and enhanced electrochemical performance.

Metal-organic frameworks (MOFs) (Chen et al., 2018; Javanbakht et al., 2019), also quoted as coordination polymers,

FIGURE 2 | The characteristics of conventional supercapacitors (SCs) like electrical double-layer capacitors (EDLCs), pseudocapacitors, and hybrid capacitors (HCs).

are constituted of porous crystalline materials and have attracted enormous attention for a variety of applications in drug delivery (Javanbakht et al., 2019), catalyst (Nadar and Rathod, 2018), gas storage and separations (Li et al., 2014; Kang et al., 2017; Chen et al., 2018), as well as sensors (Chocarro-Ruiz et al., 2018; Ko et al., 2018). Recently, they have been reported as electrode active materials with great promise for ESSs, especially for SCs. This is attributed to the ultra-large surface areas ($\sim$10,000 m^2 g^{-1}), tunable pore sizes, various structures, and diverse functionalities (Schoenecker et al., 2012; Senkovska and Kaskel, 2014; Genesio et al., 2018; Ding et al., 2019). More significantly, MOFs are a type of bifunctional materials, which can be directly applied as both electrode active materials and templates to synthesize various nanostructures for electrochemical applications. Favorable products with desired structures could be generated through tuning the synthesis methods of MOFs. Taking pristine MOFs for example, the performance is determined by its physical properties such as the conductivity, particle size, specific surface area, as well as the distribution of internal pore size (Xia et al., 2015). Notably, during the electrochemical process, it has a preferable ionic transportation for loosely packed MOFs.

Besides these fascinating features of MOFs, electrical conductivity has been one of the most crucial challenges for their wide applications as most MOFs have been characterized by low electrical conductivity (10^{-8}–10^{-6} S m^{-1}) or even insulators ($<10^{-8}$ S m^{-1}). Hence, great efforts have been made to explore highly conductive MOF nanomaterials for further applications. Generally, the conductivity is limited by charge carriers; the higher charge mobility of the charge carriers, the higher electrical conductivity of MOFs. To date, several approaches have been developed to enhance the conductivity of porous MOFs, namely, formation of composite and post-synthetic modification (Sengupta et al., 2016; Meng et al., 2019). The electron mobility of MOFs could be improved by careful and precise selection of metal clusters and organic linkers, in which the constructed architecture could exhibit long-range charge delocalization through resonance or Π–Π stacking (Sun et al., 2013; Sun et al., 2015; Clough et al., 2017; Sun et al., 2017). Another potential and versatile approach is guest doping through either introducing guest molecules or other nanomaterials with excellent conductivity (Allendorf et al., 2015; Lin et al., 2018; Xie et al., 2020).

To date, more than 20,000 types of MOFs (Furukawa et al., 2013) have been explored in various fields, and the numbers are ever increasing. However, there are three main issues associated with MOFs that need to be addressed for effective applications as electrode active materials in SCs: (1) low stability (thermal, mechanical, chemical, and water stability), (2) poor conductivity, and (3) inferior specific energy density. In terms of the stability, it could be solved through creating hydrophobic interface (Yang et al., 2011). Due to the environmental concerns, the electrolytes for most SCs are water-based. As the electroactive materials are immersed in the electrolyte, substitution reactions might occur and result in the dissociation of MOFs, in which the water molecules or hydroxide would replace metal-coordinated ligands. Therefore, strengthening the coordination bonds
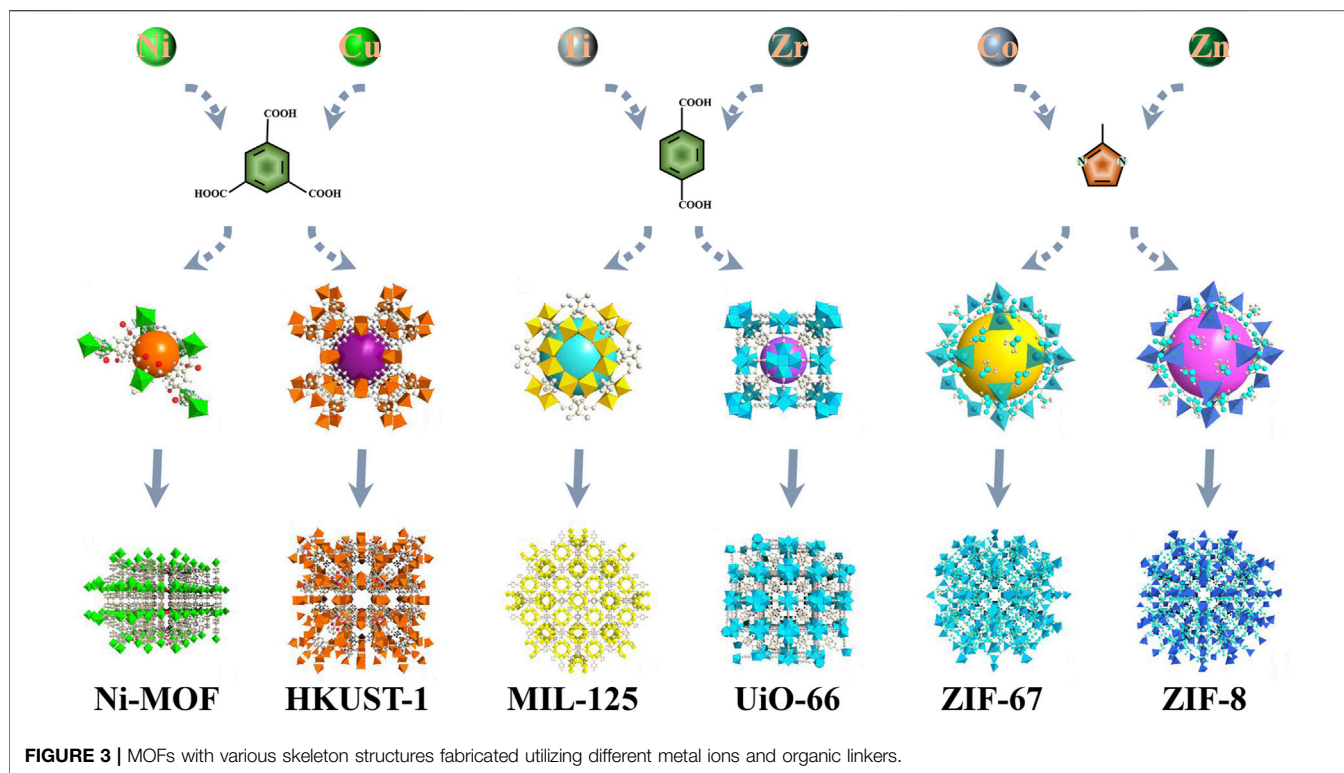
between organic linkers and secondary building units (Yang et al., 2019) is another possible option. In addition, water stability of MOFs could be improved by modifying the surfaces of MOFs and their derivatives (Yang and Park, 2012; Shih et al., 2017). Furthermore, it is challenging to fabricate high acid/base stabilized MOFs as serious degradation on the pristine structure of MOFs might be encountered under the strong acidic or alkaline conditions. According to hard and soft (Lewis) acids/bases principles, hard acids/bases have a tendency to combine with hard bases/acids (h-h), while soft acids/bases prefer to bind to soft bases/acids (s-s) instead. The orbital and charge interactions are much stronger than that of either hard Lewis acids to soft bases or hard Lewis bases to soft acids (h-s). At the same time, the molecules are going to restrict the change of pH in a buffer solution when an acid/base is added. In this case, it is hence imperative to establish a proper strategy for enhancing the stability of MOFs in acidic/alkalescent solutions as they are composed of both acidic and alkaline functional groups (Gong et al., 2016; Yang et al., 2017; He et al., 2018).

In addition, MOF-derived carbon is another attraction in the field of ESSs by reason of the high porosity, conductivity, and stability. In general, carbon is one of the earliest and most used SC electrode active materials because of the natural abundance and low cost. Meanwhile, it possesses the advantages of excellent controllability, large surface area, and chemical stability; it hence becomes an ideal choice for ESSs. Recently, the emergence of CNTs (Cao et al., 2019a; Zhou Q. et al., 2019; Li and Xu, 2019) has provided new opportunities in electrochemical energy storage, as they exhibit excellent electrical conductivity (Herren et al., 2019; Kong et al., 2019), high specific surface areas (Kim et al., 2013; Yao et al., 2015), and tunable architectures (Wang et al., 2017c; Qin R. et al., 2019). The potential and application prospects of CNTs as electrode active materials for SCs hence have been studied intensively in recent years.

Over the past two decades, various methods have been adopted for applying porous MOFs and carbonaceous materials in electrochemical ESSs. In this review, the applications of MOF materials as SC electrode materials were discussed in two aspects: (1) the performance of pristine MOFs, which are employed directly as electrodes for SCs; and (2) the applications of nanoporous composites derived from MOFs (MOF-derived carbons). Moreover, the electrochemical performance of CNT nanocomposites as SC electrode active materials are reviewed comprehensively as well.

THE APPLICATION OF PRISTINE MOF NANOMATERIALS IN SCS

To date, there are plenty of MOF-based materials that have been developed and employed in miscellaneous fields. For instance, they can be utilized for gas separation and adsorption, photocatalysts, drug delivery, etc. (Campagnol et al., 2014; Stassen et al., 2015; Denny et al., 2018; Javanbakht et al., 2019; Liu et al., 2021a). Nonetheless, although MOFs composed of high-valence transition metal ions are viewed to exhibit high stability (Cavka et al., 2008; Li et al., 2016) and superior

FIGURE 3 | MOFs with various skeleton structures fabricated utilizing different metal ions and organic linkers.

electrochemical performance (Yan et al., 2016; Wang et al., 2018), only limited literatures have been reported on these unique features. In principle, the electrochemical performance of SCs is significantly influenced by the selection of electrode materials, in which the MOF-based materials are found to exhibit a number of intriguing capabilities such as high porosity, excellent electrical conductivity, and large Brunauer-Emmett-Teller (BET) specific surface area. Besides, the selection of metal cations and organic ligands are also significant as the different connections between metal ions and organic linkers could lead to the formation of different porous architectures (as illustrated in **Figure 3**). Herein, the electrochemical performances of these nanocomposites are summarized in terms of (1) pristine MOFs that are exploited directly after being synthesized through various approaches, and (2) pyrolysis of MOFs to carbon nanomaterials with favorable intrinsic properties such as good conductivity and high stability (Bao et al., 2016; Huang et al., 2019; Yang et al., 2020).

The Electrochemical Performance of Pristine MOFs

High-valence metal ions such as Zr^{4+}, Cr^{3+}, and Fe^{3+} are usually viewed as favorable cations to form stable coordination bonds among the resulting MOF materials since they possess high coordination numbers and charge densities (Liu L. et al., 2018; Sundriyal et al., 2018; Wang et al., 2020b). There are a number of studies that have been conducted on low valence-based MOFs, such as Mn^{2+}, Cu^{2+}, Zn^{2+}, Co^{2+}, and Ni^{2+} (Kannangara et al., 2019; Sundriyal et al., 2019; Wang et al., 2020c; Ma et al., 2021a). Nonetheless, majority of pristine MOF materials are found to

exhibit low electrical conductivity and unstable structures during the long-term charging and discharging cycling. **Figure 4** indicates a comprehensive development timeline of the synthesis methods developed for the synthesis of MOFs in the past two decades (Olajire, 2018). In this review, the electrochemical performances of some prominent examples in the latest few years are systematically summarized, the critical characteristics for MOFs to achieve remarkable electrochemical properties are discussed as well.

UiO-66, a Zr-based MOF, has been studied recently as an electrode material for electrochemical capacitors, owing to its unique stability feature in aqueous environment (Liu X. et al., 2015; Lv et al., 2019; Shi et al., 2020). Nonetheless, the potential of the Zr-based MOFs as effective electrode material is greatly hampered by its low electrical conductivity and microporous structure with limited ion mobility (Goswami et al., 2018; Ray et al., 2021). Hence, to tackle these shortcomings, the UiO-66 nanomaterial with a hierarchical porous architecture was prepared through a solvothermal method at atmospheric pressure (**Figure 5**). (Gao et al., 2017) A calculated electrochemical capacitance at $0.2 \, A \, g^{-1}$ was $849 \, F \, g^{-1}$ in 6 M KOH, significantly higher than the bare UiO-66 material ($101.5 \, F \, g^{-1}$) with microporous structure. This clearly indicated that the hierarchical porous structure was befitting to greatly improve the electrochemical performance of UiO-66. The unique architecture was not only able to enlarge the specific surface area and volume, and it has also shortened the ionic migration distance and decreased the diffusion resistance in-between the KOH and reactive sites of the electrode materials. As a result, the hierarchical porous structure is essential to ensure unimpeded
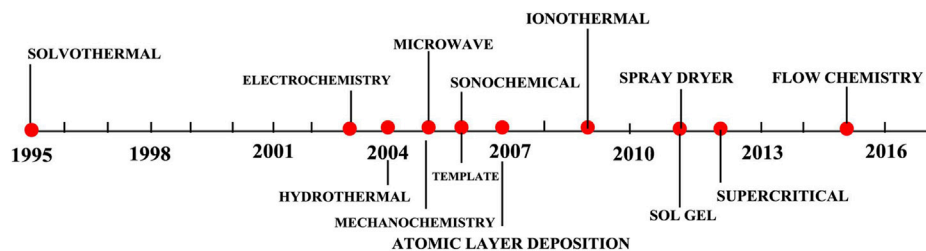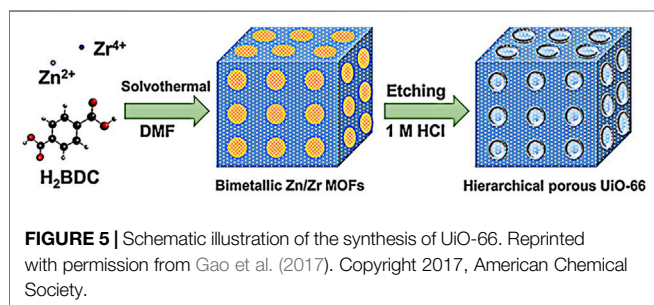
FIGURE 4 | Timeline of the synthesis methods developed for the synthesis of MOFs in the past two decades. Adapted with permission from (Olajire, 2018). Copyright 2018, Elsevier.

FIGURE 5 | Schematic illustration of the synthesis of UiO-66. Reprinted with permission from Gao et al. (2017). Copyright 2017, American Chemical Society.
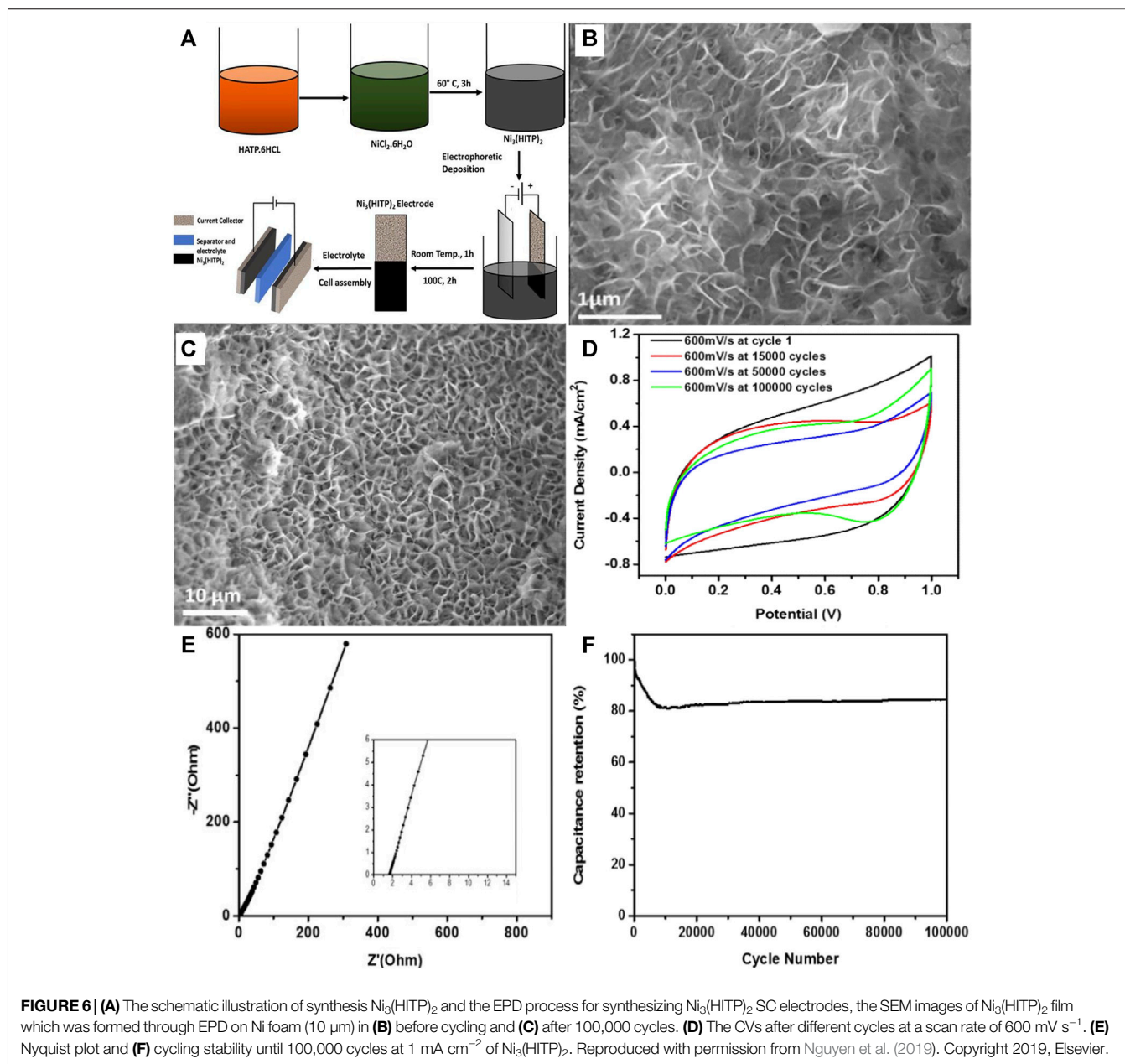
channels for charge transfer process to take place and speed up the redox process.

Another similar study was conducted by Tan et al. (2015) with improved properties, while Zr-MOFs were synthesized without the addition of $Zn(NO_3)_2$. It delivered an electrochemical capacitance of 1,144 F g^{-1} at 5 mV s^{-1}, which was considerably higher than that of UiO-66 (Gao et al., 2017). This was ascribed to two main reasons. Firstly, the homogeneous Zr-MOFs with small particle sizes of 100 nm could be beneficial to enhance the BET surface area, which was 1,047 m^2 g^{-1}. Such high surface area could efficiently store a large number of charges and eventually improved the capacitive performance. Secondly, the 3D structure of Zr-MOFs could reduce the diffusion resistance of the electrolyte and provide smooth channels for ion transport, since the recorded internal resistance (R$_s$) was only 0.42 Ω. More importantly, at 10 mV s^{-1} after 2,000 cycles in alkaline environment, it could maintain 57.2% of its starting capacitance, suggesting the high stability of the electrode active materials.

Besides, MOFs with low-valence cations are found to possess excellent capacitive capability and cyclability as well. For example, cobalt and nickel offer abundant redox-active sites and are readily to be employed for developing MOFs with good electrochemical performance. Cobalt-based coordination polymer with outstanding performance was synthesized through a facile synthesis route (Yang et al., 2017). An excellent electrochemical capacitance of 2,564 F g^{-1} at a current density of 1 A g^{-1} in 5 M KOH was recorded, and it could still achieve a capacitance of 1,164 F g^{-1} when the rate was enlarged to 20 A g^{-1}, revealing the outstanding rate performance of the Co-MOF materials. There were three rationalizations that led to the electrochemical performance improvement. First and foremost, the existence of a large number of thin nanosheets has

contributed to significant surface area enhancement. The large surface area was not only feasible to offer sufficient contact between electrode active materials and electrolyte; it had also shortened the migration distance of OH$^-$. Besides, the as-synthesized Co-MOFs with a high conductivity of 3.75 × 10^{-3} S cm^{-1} could speed up the charge transfer in the interface between electrolyte and electrode, and eventually enhanced the specific capacitance. Furthermore, the large volume between interlayers, which were formed on the bc plane through the interaction of Co-O-Co chain and the double chains of CoO$_6$, were capable to store electrolytes and improve the intercalation and de-intercalation efficiency of OH$^-$. In addition, it exhibited a desired cycling stability where a maximum capacitance retention of 95.8% was obtained after 3,000 continuous charging and discharging cycles at 2 A g^{-1}. The extraordinary cycling stability could be attributed to the unique layered structure with conductive network frames, in which the existence of terephthalate groups between the layers could serve as supportive pillars to avoid the collapse of the architecture.

Nickel-based MOFs have been widely explored as they are viewed to exhibit high electrolyte compatibility, excellent electrochemical performance and ultrahigh conductivity [up to 800 S m^{-1} (Dou et al., 2017)]. For instance, Nguyen and co-workers developed ultrathin 2D Ni$_3$(2,3,6,7,10,11-hexaaminotriphenelene)$_2$ {Ni$_3$(HITP)$_2$} via electrophoretic deposition (EPD) (Nguyen et al., 2019). The relevant synthesis process and electrochemical properties are illustrated in **Figure 6A**. At a scan rate of 0.1 mA cm^{-2} in 0.5 M Na$_2$SO$_4$, the areal capacitance of the as-obtained MOF material was 15.69 F cm^{-2}. The superior capacitive performance was ascribed to the 3D porous Ni$_3$(HITP)$_2$ with micrometer-large pores (**Figures 6B,C**), in which the large pore sizes could offer enough interspace to store electrolyte and boost ion transport. Moreover, the electrode active material has shown an excellent capacitive behavior with high electrical conductivity, since the cyclic voltammetry (CV) curve with a closely quasi-rectangular shape was sustained at a very high rate of 4,000 mV s^{-1}. More crucially, the structure of the active material was ultra-stable; approximately 84.14% of the starting capacitance was maintained over 100,000 charging and discharging cycles (**Figures 6D,F**) at a low rate of 1 mA cm^{-2}. This was caused by the layer-by-layer nanosheets and the electrical double-layer capacitive behavior. Meanwhile, a low R$_s$ of 1.47 Ω was recorded (**Figure 6E**), which might be elucidated by two factors: (1) the layer-by-layer

FIGURE 6 | (A) The schematic illustration of synthesis $Ni_3(HITP)_2$ and the EPD process for synthesizing $Ni_3(HITP)_2$ SC electrodes, the SEM images of $Ni_3(HITP)_2$ film which was formed through EPD on Ni foam (10 μm) in **(B)** before cycling and **(C)** after 100,000 cycles. **(D)** The CVs after different cycles at a scan rate of 600 mV s^{-1}. **(E)** Nyquist plot and **(F)** cycling stability until 100,000 cycles at 1 mA cm^{-2} of $Ni_3(HITP)_2$. Reproduced with permission from Nguyen et al. (2019). Copyright 2019, Elsevier.

nanosheets of $Ni_3(HITP)_2$ without any addition of binder, and (2) nanopores on the structure shortened electrolyte diffusion distance. This was among the most superior cycle life that has been reported on MOF-based SCs.

It is also possible to employ Ni-MOFs as all-solid-state SCs since wearable device is another attraction in the application of electrochemical ESSs. Generally, all-solid-state SCs exhibit a relatively lower capacitive performance and cyclic stability due to the utilization of limited electrolyte as compared to normal SCs (Cheng et al., 2019). Recently, a layered nanosheet Ni-MOF was developed and utilized for flexible solid-state SC (Yang et al., 2020). The electrode material has shown a high electrochemical capacitance of 1,518.8 F g^{-1} at 1 A g^{-1}, and a good rate performance of 483.3 F g^{-1} at a current density of 20 A g^{-1}.

Meanwhile, an outstanding capacitance retention of 95.5% over 10,000 cycles at 20 A g^{-1} was reported. These ultra-high electrochemical performances could result from the following factors: (1) The stable structure of Ni-MOFs in alkaline environment. (2) The large space offered between layers was beneficial to store electrolyte and enhance the facile intercalation and de-intercalation of OH$^-$. (3) Unit cells were formed along the bc plane, essential in improving the transport of electron and diffusion of electrolyte. The electrochemical performance of some pristine MOFs commonly employed as SC electrode materials is illustrated in **Table 1**.

As a summary, the architectures of the synthesized MOFs have a crucial role to play in the electrochemical-related properties; it is hence necessary to understand the interactions between the active

TABLE 1 | The summary of the electrochemical performance of pristine MOFs materials utilized as SCs electrode materials.

Material	Capacitance at scan rate/Current density	Electrolyte	Potential window (V)	Reference electrode	Capacitance retention (%)/Cycle number	References
Supercapacitor						
UiO-66(Zr)	101.5 F g^{-1} at 0.2 A g^{-1}	6 M KOH	0.6	Hg/HgO	—	Gao et al. (2017)
UiO-66(Zr)	1,144 F g^{-1} at 5 mV s^{-1}	6 M KOH	0.75	SCE	57.2/2,000	Tan et al. (2015)
MOF-867	5.085 mF cm^{-2} at 5 mV s^{-1}	—	2.7	—	92/10,000	Choi et al. (2014)
Cu-LCP	1,274 F g^{-1} at 1 A g^{-1}	1 M LiOH	0.5	SCE	88/2,000	Liu et al. (2015a)
	568 F g^{-1} at 20 A g^{-1}					
Cu-MOF	1,148 F g^{-1} at 0.5 A g^{-1}	6 M KOH	0.5	SCE	90/2,000	Xiong et al. (2017)
Mn-MOF	443 F g^{-1} at 1 A g^{-1}	6 M KOH	0.5	SCE	86/1,000	Feng et al. (2020)
Mn-MOF	1,098 F g^{-1} at 1 A g^{-1}	1 M KOH	0.45	SCE	92.6/2,000	Wang et al. (2017b)
	396 F g^{-1} at 20 A g^{-1}					
	1,178 F g^{-1} at 1 A g^{-1}	1 M LiOH	0.5	SCE	94.6/2,000	
	425.26 F g^{-1} at 20 A g^{-1}					
Mn-MOF	10.25 F cm^{-2} at 2 A g^{-1}	2 M KOH	0.6	Hg/HgO	92.6/5,000	Shinde et al. (2020)
	5.72 F cm^{-2} at 12 A g^{-1}					
Mn-MOF	371 F g^{-1} at 0.5 A g^{-1}	6 M KOH	0.6	Hg/HgO	—	Xu et al. (2019)
	248 F g^{-1} at 10 A g^{-1}					
Mn-BDC MOF	64.5 F g^{-1} at 0.25 A g^{-1}	PVA-1 M Na$_2$SO$_4$	1.5	Ag/AgCl	98/2,000	Sundriyala et al. (2019)
Co-MOF/NF	13.6 F cm^{-2} at 2 mA cm^{-2}	2 M KOH	0.8	Hg/HgO	47/10,000	Zhu et al. (2018)
Co-MOF	952.5 F g^{-1} at 0.25 A g^{-1}	3 M KOH	0.5	Ag/AgCl	85/2,000	Xuan et al. (2018)
Co-MOF	958.1 F g^{-1} at 2 A g^{-1}	3 M KOH	0.5	Ag/AgCl	92.3/3,000	Ramachandran et al. (2018)
Co-MOF	2,564 F g^{-1} at 1 A g^{-1}	5 M KOH	0.35	SCE	95.8/3,000	Yang et al. (2017)
	1,164 F g^{-1} at 20 A g^{-1}					
Ni-MOF	1,057.2 F g^{-1} at 1 A g^{-1}	3 M KOH	0.4	SCE	75/2,500	Du et al. (2018)
	649 F g^{-1} at 30 A g^{-1}					
Ni$_3$(HAB)$_2$	13.65 F cm^{-2} at 0.1 mA cm^{-2}	0.5 M Na$_2$SO$_4$	1	—	81.2/50,000	Wechsler and Amir, (2020)
Ni$_3$(HITP)$_2$	15.69 F cm^{-2} at 0.1 mA cm^{-2}	0.5 M Na$_2$SO$_4$	1	—	84.14/100,000	Nguyen et al. (2019)
Ni-MOF	1,518.8 F g^{-1} at 1 A g^{-1}	2 M KOH	0.5	—	95.5/10,000	Yang et al. (2020)
	483.3 F g^{-1} at 20 A g^{-1}					
Hybrid Capacitor						
Mn-MOF//rGO	211.4 F g^{-1} at 5 A g^{-1}	2 M KOH	1.5	Hg/HgO	81.18/10,000	Shinde et al. (2020)
	131.07 F g^{-1} at 40 A g^{-1}					
Mn-MOF// graphene	89 F g^{-1} at 1 A g^{-1}	6 M KOH	1.6	Hg/HgO	91.8/10,000	Xu et al. (2019)
Zn-MOF//AC	140.8 Wh kg^{-1} at 70.0 W kg^{-1}	2 M ZnSO$_4$	1.6	—	72/20,000	Wang et al. (2019)
	46.6 Wh kg^{-1} at 2,850 W kg^{-1}					
Zn-pPDA MOF-5//GC	62.75 Wh kg^{-1} at 4,501.1 W kg^{-1}	1 M KOH	1.5	Ag/AgCl	96.2/2,000	Kannangara et al. (2019)
Zn-pPDA MOF-8//GC	57.52 Wh kg^{-1} at 4,499.03 W kg^{-1}				96.81/2,000	
Zn-pPDA MOF-12//GC	52.25 Wh kg^{-1} at 4,498.92 W kg^{-1}				96.79/2,000	
Ni-MOF//AC	244 mF cm^{-2} at 0.5 mA cm^{-2}	KOH-PVA	1.5	—	97.2/2,000	Yang et al. (2020)

materials and electrolyte. Meanwhile, the other factors, including morphology, pore size, and porous structure, also need to be taken into consideration when selecting a core electrode material for SCs. These factors could substantially influence the diffusion rate of electrolyte and therefore affect the lifespan of the device.

The Electrochemical Performance of MOF-Derived Carbon Nanocomposites

Apart from the direct utilization of pristine MOFs, MOF materials have been employed as precursors to derive various carbon compounds. In recent years, carbonaceous materials, developed through direct carbonization from organic materials, have been widely investigated as electrochemical energy storage units, like fuel cells (You and Kamarudin, 2017), batteries (Yi-Ju et al., 2019), and SCs (Chang et al., 2017) due to their nontoxicity and excellent electrical conductivity. However, their potential applications are greatly limited by the low surface areas, non-uniform particle sizes, and chaotic structures (Wang C. et al., 2017). Therefore, to tackle these shortcomings, MOF-derived carbon nanocomposites with nanoporous architectures and ultra-large ionic accessible surface

areas have been synthesized (Cao et al., 2017). Micro- and mesoporous carbonaceous materials such as graphene, AC, and CNTs have a significant role to play in SCs, since the large interspace offered is befitting to store enough electrolyte and shorten the diffusion path for ionic transportation (Bonaccorso et al., 2015). Besides, the *in situ* heteroatoms doping (such as P, F B, N, and S) in the prepared carbonaceous nanocomposites could be facilely achieved by selecting suitable MOF precursors, while the electrical conductivity, cyclability, and capacitive performance can be enhanced by the introduction of heteroatoms into highly nanoporous carbons (NPCs) due to the synergistic effect (Dai et al., 2018b; Gao et al., 2018; Ma et al., 2018; Kim et al., 2019). As MOF materials have a wide range of applications owing to their unique structures, MOF-derived carbons have also expanded their potential applications in SCs.

NPCs can be obtained from MOFs through a simple heat treatment, and these active materials often exhibit micro/mesoporous architectures and large specific surface areas, which are crucial characteristics to optimize the electrochemical performance for SCs. Thus, the as-derived carbon materials could have good electrochemical performance. NPC with interconnected hierarchical meso- and micro-porous architecture was synthesized by Chang's team (Chang et al., 2017). The obtained capacitive performance was 425 F g^{-1} when the current density was 2 A g^{-1} in 1 M H_2SO_4, which was almost twice of MOF-derived TMOs (Liu Q. et al., 2015; Wang et al., 2017b). The capacitance was recorded as 244 F g^{-1} (57.4%) when the current density was increased up to 10 A g^{-1}, which clearly indicated the good rate capability of MOF-525-derived NPC. The high capacitance could be caused by the pseudo-capacitance of functional groups and unique structure. Firstly, oxygen-containing groups, forming during the process of pyrolysis, were not only beneficial to generate pseudo-capacitance, but also enhanced the wettability of active materials. Nitrogen-containing functional groups could be responsible for the redox pseudo-capacitance due to the existence of pyridinic and pyrrolic groups. Secondly, the hierarchical micro- and meso-porous architecture with a large number of sp^2 bonded carbon accelerated the diffusion of ions and eventually enhanced the capacitive performance. Lastly, it provided a large specific surface area of 786 m^2 g^{-1}, which provided sufficient electroactive sites for charge transport and interactions.
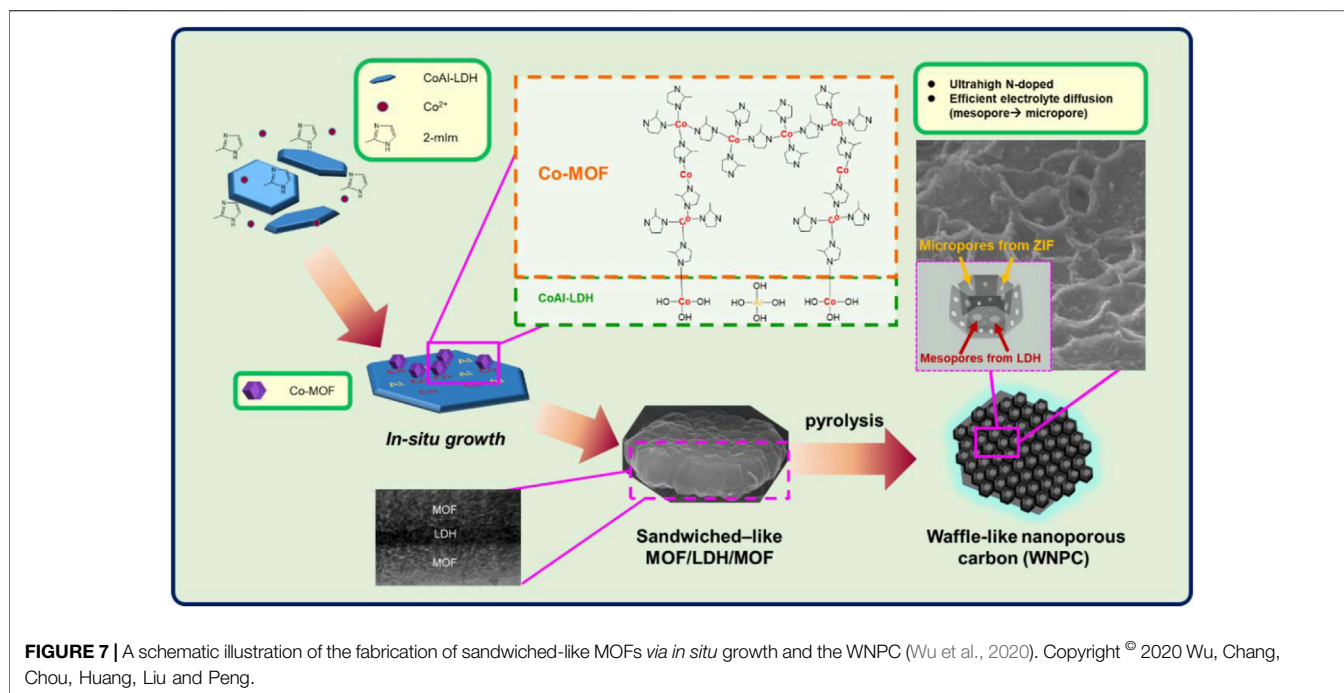
NPC could also be obtained from Zn-MOF at 800°C, and the performance was tested under the same condition, while it was mixed with 20% PVDF in *N*-methyl-2-pyrrolidone (NMP) as binder (Salunkhe et al., 2014). As the obtained material was fabricated into electrode for SCs, it delivered an electrochemical capacitance of 251 F g^{-1} at a scan rate of 5 mV s^{-1}. Meanwhile, there was a capacitance retention of approximately 50% as a high rate of 1,000 mV s^{-1} was employed, which evidently revealed the excellent transport and conductive properties of the electrode. This was mainly ascribed to the high content of nitrogen (15%) and ultra-large BET specific surface area of 1,523 m^2 g^{-1}, because of the special microporous architecture, in which NPC exhibited uniform and symmetric geometry with polyhedral morphology.

Additionally, it could maintain 92% of its original capacitive performance after 2,000 charging/discharging cycles at 7.5 A g^{-1}, indicating a relatively great cyclic stability.

The electrochemical property of MOF-derived carbon can be further improved by the addition of heteroatoms that are derived from organic ligands. These heteroatoms are able to strengthen the interactions between ions and surfaces, which is beneficial to stabilize the porous structures. For instance, NC900, nanoporous nitrogen-doped carbon, was developed by heating its precursor, Cd-MOF {Cd(NIPA) (CH$_3$CH$_2$OH)$_3$, NIPA: 5-nitroisophthalic acid}, at 900°C (Wang Y. et al., 2020). The as-obtained electrode possessed a specific capacitance of 367 F g^{-1} at 1 A g^{-1} and an efficiency of 95% was retained after 3,000 cycles in a three-electrode system, suggesting the nanoporous structure exhibited an excellent stability. Meanwhile, low R$_s$ of 0.43 Ω and charge transfer resistance (R$_{ct}$) of 4.57 Ω were recorded in the same study. The enhanced electrochemical performance was attributed to a nanostructure with an average pore size of 800 nm, which effectively improved the diffusion rate of electrolyte and offered higher number of active sites. In addition, when NC900 was employed to assemble an SC cell, it possessed a specific capacitance of 46 F g^{-1} at 0.5 A g^{-1} within a potential window of 1.6 V, while the energy and power densities were recorded as 6.3 Wh kg^{-1} and 246.9 W kg^{-1}, respectively. After charging and discharging 1,000 cycles at 0.5 A g^{-1}, a high retention of 96% was obtained.

In another study, waffle-like nanoporous carbons (WNPC) were synthesized (**Figure 7**) with high contents of nitrogen (7.5 wt%) and oxygen (9.1 wt%) and the electrochemical property of this material was tested in a three-electrode configuration using 1 M H_2SO_4 (Wu et al., 2020). During the electrochemical test, the CV curves of WNPC delivered a pair of redox peaks, which might arise from the pseudo-capacitance of doped oxygen and nitrogen molecules. In the meantime, the electrode presented a capacitance of 300.7 F g^{-1} at 1 A g^{-1} and retained 72% of its initial capacitance at a current density of 20 A g^{-1}, which was higher than that of NPC, suggesting the fast electrode kinetics. Moreover, the efficiency loss was only 13% after charging and discharging for 10,000 cycles at 4 A g^{-1} within an operating voltage window of 0–1 V (vs. Ag/AgCl), indicating the excellent cyclic stability. Such outstanding performance was ascribed to the existence of micro- and mesopores, in which the mesopores were able to accelerate ionic diffusion, while micropores offered a large BET surface area of 594 m^2 g^{-1}. As WNPC was fabricated into SC electrode in 1 M organic electrolyte (TEABF$_4$), the working potential was changed to 1.5–2.5 V in a two-electrode system. It was found that this device possessed an energy density and power density of 27 Wh kg^{-1} and 500 W kg^{-1} at 0.5 A g^{-1}. Even though the current density was increased up to 4 A g^{-1}, it was capable of maintaining a high energy and power density of 19.7 Wh kg^{-1} and 4,000 W kg^{-1}, respectively. Furthermore, the excellent capacitance retention was just 2% lower than that in aqueous electrolyte over the identical current density, showing the favorable stability of WNPC.

Additionally, the stability of carbon derived from MOF materials for SC electrodes can be further enhanced through

FIGURE 7 | A schematic illustration of the fabrication of sandwiched-like MOFs *via in situ* growth and the WNPC (Wu et al., 2020). Copyright © 2020 Wu, Chang, Chou, Huang, Liu and Peng.
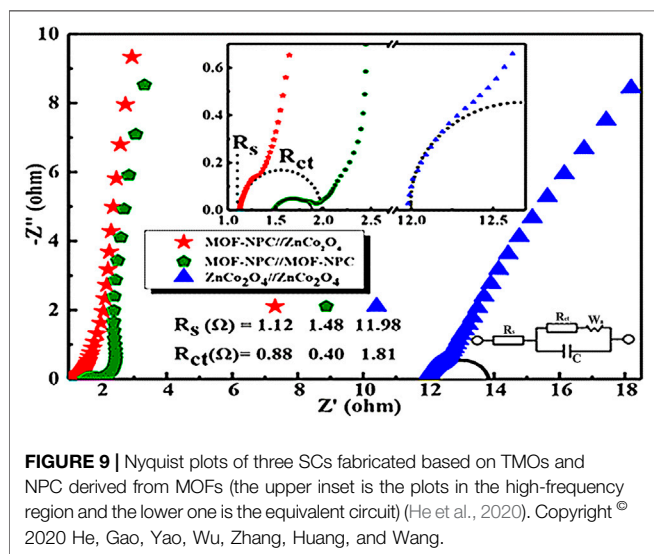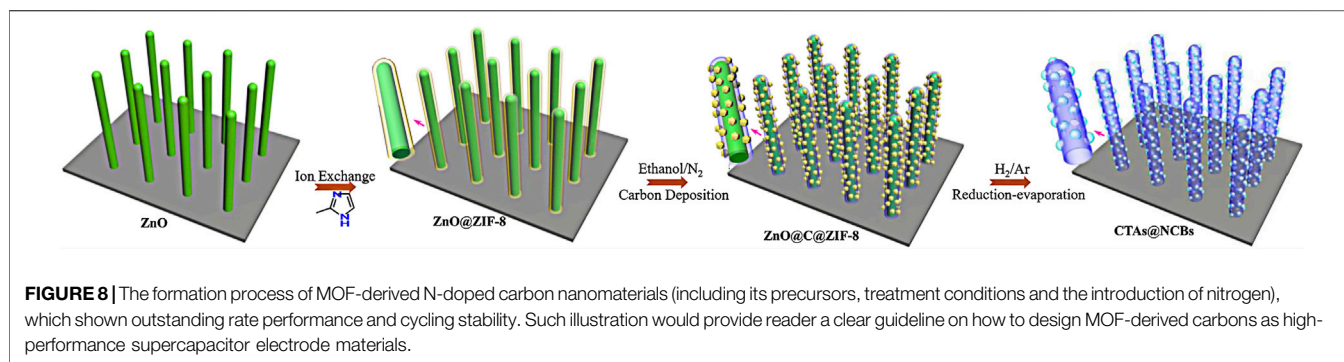
precise control of the structural pore size. For example, Liu and co-workers (Liu et al., 2021c) have synthesized ultra-microporous carbon nanoparticles from UiO-67 at a slightly low carbonizing temperature (750°C). The as-derived carbon was characterized with a pore size of 0.53 nm and a BET-specific surface area of 843 $m^2 g^{-1}$. Meanwhile, the recorded specific electrochemical capacitance of 256 $F g^{-1}$ at 1 $A g^{-1}$ in 6 M KOH was obtained, and the as-fabricated electrode could retain 91% of its starting value after 10,000 charging/discharging cycles at 2 $A g^{-1}$. Hierarchically ultra-micropore and packing mesopore structure, which might lead to fast ion transfer and reduction of diffusion path, was the most dominant characteristic that is able to ameliorate the capacitive performances of the electrode.

Through rational designs, 3D hybrid-hierarchical porous carbon with high ionic accessible surface area and long-term cyclic stability was obtained from zeolitic imidazolate framework (ZIF)-8 (Bao et al., 2016). The derived hybrid-porous carbon displayed a high BET-specific surface area of 1,056.8 $m^2 g^{-1}$ and a pore volume of 0.693 $cm^3 g^{-1}$, resulting from both interconnected micro- and mesopore structures. Meanwhile, the electrochemical behavior was tested in a three-electrode configuration in 6 M KOH electrolyte solution. The acquired specific capacitance was 215 $F g^{-1}$ at 5 $A g^{-1}$ for this electrode. Most notably, this value was found to maintain at 100% even after 10,000 cycles under the same current density. The extraordinary stability was attributed to the micropore structures that able to facilitate the short distance between the surface of electrode and center of ions and hence boosted both charge and electrolyte transfer effectively. Simultaneously, macropore structures also offered an alternative channel for electrolyte ions to access the double-layer capacitive carbon materials, improving the electrode kinetics and the rate of electrochemical reactions.

It is also possible to employ MOF-derived carbon for flexible SCs. For example, N-doped carbon nanostructures with a specific surface area of 905 $m^2 g^{-1}$ were developed (**Figure 8**) by Tang et al. (2018). The large surface area was attributed to the co-existence of meso- and micropores. The acquired electrochemical capacitance was 244 $F g^{-1}$ at 0.67 $A g^{-1}$ and 139 $F g^{-1}$ (56.97%) at an ultra-high current of 134 $A g^{-1}$ within 0–1 V (vs. Hg/Hg$_2$SO$_4$). Additionally, the capacitance retention was as high as 98.5% over 10,000 charging and discharging cycles at a current density of 20 $mA cm^{-2}$, suggesting the preferable electrochemical cyclic stability of N-doped MOF-derived carbon. The excellent capacitive performances were ascribed to three factors: (1) The binder-free carbon electrode reduced the interfacial resistance. (2) Micropores could provide large surface area and mesopores facilitated low-resistant ion transport channels for electrolyte. (3) The doped nitrogen atoms not only speeded up the kinetics of ion diffusion and transport of charges, but also enhanced the wettability and conductivity of the as-developed carbon materials.

Apart from symmetrical SCs, HCs with improved energy density without fading their power density have been widely explored. Through an "all in one" strategy, both NPCs and bimetallic oxides (ZnCo$_2$O$_4$) were obtained from the same precursor (He et al., 2020). The as-synthesized samples were analyzed in terms of pore size distributions. In the adsorption isotherm analysis, both NPC and TMO (ZnCo$_2$O$_4$) exhibited hierarchical porous architectures with macro-, meso-, and micropores. Hence, the BET surface areas of NPC and ZnCo$_2$O$_4$ were recorded at 1,137 and 440 $m^2 g^{-1}$, respectively, confirming that TMOs and NPC with a nanoporous structure could be obtained from the single precursor MOF. Meanwhile, ZnCo$_2$O$_4$ and NPC were recorded with a high capacitive performance of 420 $F g^{-1}$ and 270 $F g^{-1}$, respectively. The

FIGURE 8 | The formation process of MOF-derived N-doped carbon nanomaterials (including its precursors, treatment conditions and the introduction of nitrogen), which shown outstanding rate performance and cycling stability. Such illustration would provide reader a clear guideline on how to design MOF-derived carbons as high-performance supercapacitor electrode materials.

FIGURE 9 | Nyquist plots of three SCs fabricated based on TMOs and NPC derived from MOFs (the upper inset is the plots in the high-frequency region and the lower one is the equivalent circuit) (He et al., 2020). Copyright © 2020 He, Gao, Yao, Wu, Zhang, Huang, and Wang.

enhanced electrochemical properties could be ascribed to the hierarchically porous architectures where micropores were employed to accumulate ions while mesopore structures could improve the transfer of the ions. When HC (NPC//$ZnCo_2O_4$) was assembled by employing binary TMOs as cathode and NPC as anode, it delivered a maximum energy density of 28.6 Wh kg^{-1} at 100 W kg^{-1} within a broad electrochemical potential window of 0–1.45 V (vs. Hg/HgO) in 6 M KOH. An energy density of 18 Wh kg^{-1} was achieved when the power density was increased up to 2.5 kW kg^{-1}. As shown in **Figure 9**, a low R$_s$ of 1.12 Ω was obtained, which was lower than that obtained from both NPC and TMOs-based SCs.

The electrochemical properties of some MOF-derived carbons utilized as SC electrode materials are summarized in **Table 2**. The recent trends in utilizing MOFs as precursors to derive highly porous carbonaceous materials evidently prove that it is one of the most effective strategies to achieve tremendous electrochemical performance. Also, it is obvious that the pore size distribution on carbon-based nanomaterials is one of the dominant factors to maneuver the electrochemical performance of energy storage devices. Therefore, to reach outstanding performance, MOF-derived carbon materials should possess several important characteristics. First, to store more charges

in the interface between electrolyte and electrode, a high surface becomes significant. Second, to construct an efficient conductive network, these nanomaterials should exhibit excellent electrical conductivity. Third, to enhance its lifespan, an outstanding physiochemical property is crucial, coupled with high thermal and mechanical stability. Moreover, to enhance the energy density, heteroatom doping and/or combining with other pseudocapacitive materials are feasible. Most importantly, to facilitate the mass transport of charge carriers, a preferable range of pore size distribution is essentially critical for effective ion diffusion and storage during the electrochemical process.

THE APPLICATION OF CARBON NANOTUBE NANOCOMPOSITES IN SCS

SCs with high power density (~10^4 W kg^{-1}) and ultralong cycle life (~10^5) have become one of the most promising devices for ESSs. Nevertheless, most SCs are burdened by the low electrical conductivity and energy density. To handle these problems, great efforts have been devoted to fabricating new SC electrode materials with desired energy density as well as low cost. Carbonaceous materials, such as AC (Wang F. et al., 2020; Liu et al., 2020), graphene (Dai et al., 2018a; Manjakkal et al., 2018), carbon fibers (Ni et al., 2020; Yue et al., 2020; Li et al., 2021; Jiang et al., 2021), and CNTs (Wang et al., 2014; Zou et al., 2018; Cao et al., 2019b) with preferable conductivity and stability, have been widely investigated for SC electrodes. Among these carbon-based electrode active materials, CNTs with critical features like excellent electrical conductivity and controllable pore size are crucial for SCs. In addition, the electrochemical performance can be enhanced through introducing functional groups and heteroatoms on the surface of carbon-based nanomaterials (Qin T. et al., 2019; Wang et al., 2020d). This is because the integration of other nanomaterials is beneficial to significantly improve the conductivity as well as capacitive performance by reason of the synergistic effect.

The addition of CNTs not only is able to facilitate the electrical conductivity of SC electrodes but also improves the surface area and bring in carboxyl functional groups to enhance capacitive performance. For instance, CNT nanocomposites were loaded on AC to improve the electrochemical property of the as-developed
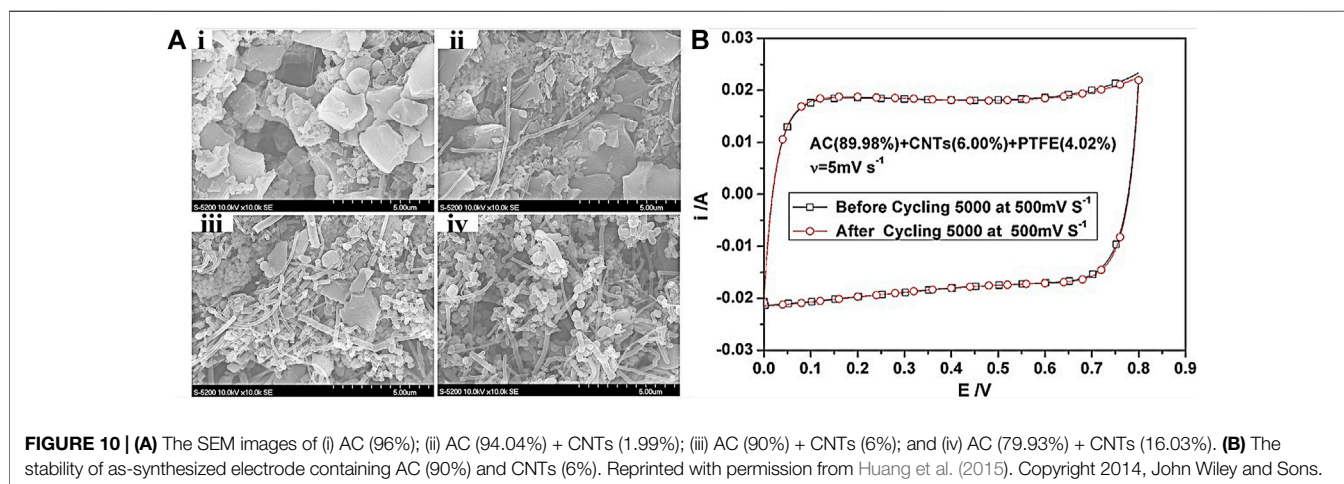
TABLE 2 | The summary of the electrochemical performance of MOF-derived carbon nanomaterials as electrode active materials for SCs.
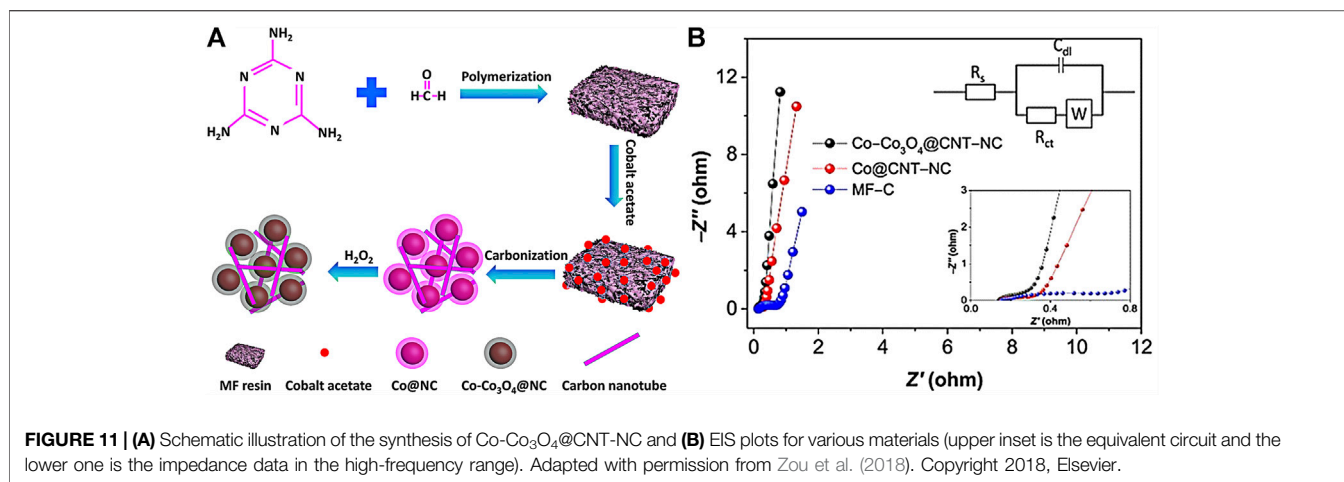
Samples	Capacitance (F g^{-1}) at scan rate/Current density	Electrolyte	Potential window (V)	References electrode	Capacitance retention (%)/Cycle number	References
NPC	425 at 2 A g^{-1} 244 at 10 A g^{-1}	1 M H$_2$SO$_4$	1	Ag/AgCl	—	Chang et al. (2017)
NPC	98 at 0.5 A g^{-1} 62 at 5 A g^{-1}	1 M H$_2$SO$_4$	0.9	Ag/AgCl	92/3,000	Salunkhe et al. (2014)
NC900	367 at 1 A g^{-1} 46 at 0.5 A g^{-1}	6 M KOH	1 / 1.6	Hg/HgO / —	95/3,000 / 96/1,000	Wang et al. (2020e)
WNPC	300.7 at 1 A g^{-1} 216.5 at 20 A g^{-1}	1 M H$_2$SO$_4$	1	Ag/AgCl	87/10,000	Wu et al. (2020)
UCNs	256 at 1 A g^{-1}	6 M KOH	1	Hg/HgO	91/10,000	Liu et al. (2018b)
Hybrid-porous C	215 at 5 A g^{-1}	6 M KOH	1	SCE	100/10,000	Bao et al. (2016)
N-doped C	244 at 0.67 A g^{-1} 139 at 134 A g^{-1}	1 M H$_2$SO$_4$	1	Hg/Hg$_2$SO$_4$	98.5/10,000	Tang et al. (2018)
PC-Zn	138 at 0.5 A g^{-1}	6 M KOH	1	SCE	91.8/5,000	Yue et al. (2018)
c-CN	333.8 at mV s^{-1}	1 M LiTFSI	1.2	Ag/AgCl	88.1/12,000	Cai et al. (2020)
ZnO/C@(Ni, Co)Se$_2$	164.18 mA h g^{-1} at 1 A g^{-1}	6 M KOH	1.4	Hg/HgO	97.87/10,000	Liu et al. (2021a)

electrodes (Huang et al., 2015). Particularly, a certain amount (0–20 wt%) of multi-walled CNTs (MWCNTs) was added into AC to fabricate SC electrode. The results indicated that the capacitive performance could be boosted as less than 10 wt% of MWCNTs was loaded, while no significant change was detected when the content of MWCNTs was more than 10 wt %. Most notably, the as-assembled SC exhibited an electrochemical capacitance of 102.5 F g^{-1} when 10 wt% of MWCNTs was used, which was approximately 15% higher than bare AC owing to the enhancement of surface area (**Figure 10A**). Unlike the capacitive performance, the conductivity, mechanical strength, and stability could be further improved when a large amount of MWCNTs was incorporated. Evidently, there was no decline of capacitance after 5,000 cycles at 500 mV s^{-1} in 4 M KOH (**Figure 10B**).

Another similar study was conducted to investigate the impact on series resistance of AC coating with low loading of MWCNTs (Lei and Lekakou, 2013). It was found that the as-developed SC obtained a specific capacitance of 180 F g^{-1} at 10 mV s^{-1}.

Meanwhile, it could maintain 90% of its initial capacitance after 5,000 cycles when 0.15% MWCNTs were utilized. The amelioration of the electrochemical properties was principally accredited to the capability of the CNTs to reduce the electrical resistivity through shortening charge transfer path due to the residue of oxygen groups. Consequently, the incorporation of CNTs could enhance both the power density and energy density of the electrode. Moreover, the simultaneous addition of functional groups and heteroatoms was able to critically improve the power density. For instance, Wang and co-workers introduced hydroquinone (HQ) into aqueous electrolyte (1M H$_2$SO$_4$) and coated redox-active molecules on the surface of CNTs (Wang et al., 2014). As a result, the as-synthesized electrode (CNTs-T) possessed a superior electrochemical capacitance of 3,199 F g^{-1} in the modified electrolyte (1 M H$_2$SO$_4$ + 0.075 M HQ) as the scan rate was 5 mV s^{-1}. Nonetheless, the retention efficiency was only 70% after 350 galvanostatic charge and discharge (GCD) cycles at 5 mV s^{-1}.

FIGURE 10 | (A) The SEM images of (i) AC (96%); (ii) AC (94.04%) + CNTs (1.99%); (iii) AC (90%) + CNTs (6%); and (iv) AC (79.93%) + CNTs (16.03%). **(B)** The stability of as-synthesized electrode containing AC (90%) and CNTs (6%). Reprinted with permission from Huang et al. (2015). Copyright 2014, John Wiley and Sons.

FIGURE 11 | (A) Schematic illustration of the synthesis of Co-Co$_3$O$_4$@CNT-NC and **(B)** EIS plots for various materials (upper inset is the equivalent circuit and the lower one is the impedance data in the high-frequency range). Adapted with permission from Zou et al. (2018). Copyright 2018, Elsevier.

Usually, hybrid carbonaceous nanomaterials with TMOs are promising electrode active materials to enhance the electrical conductivity and capacitive performance. ZnFe$_2$O$_4$-CNT (ZFO-CNT) nanocomposite electrode was synthesized through successive ionic layer adsorption and reaction method (Raut et al., 2018). It was found that ZFO-CNT electrode could deliver 217 mA h g^{-1} at 5 mV s^{-1} in 1 M KOH, and it could maintain 74.7% of the capacitance as the scan rate rose to 40 mV s^{-1}. Such outstanding capacitive performance was the prominent outcome as a result of the highly contacted area and shortened charge transfer distance provided by ZFO nanoparticles. Meanwhile, the multiple oxidation states of these two metal ions (Zn and Fe) helped to enhance the electrochemical property. To further explore the electrochemical properties, a device containing ZFO-CNTs and polyvinyl alcohol-lithium chloride (PVA-LiCl) without separator was fabricated as well (Raut et al., 2018). This device provided a specific capacitance of 92.2 F g^{-1} at 0.35 A g^{-1}. Additionally, approximately 72% of its starting capacitance was sustained over 2,000 cycles at the same current density. Furthermore, the as-synthesized device exhibited a relatively low resistance, in which the acquired R$_s$ and R$_{ct}$ were 2.09 and 0.5 Ω, respectively. These results indicated that this unique synthesis approach could directly form an electrode without the application of any binder. More significantly, the synergy effect of the nanocomposite electrode could evidently result in superior charge storage performance.

In another similar study, TMOs with N-doped carbon-based nanomaterials with improved conductivity and higher structural stability were developed (Zou et al., 2018). Specifically, a core@shell architecture of Co-Co$_3$O$_4$ core nanoparticles in CNT-incorporated N-doped carbon (Co-Co$_3$O$_4$@CNT-NC) was fabricated through a simple pyrolysis method (**Figure 11A**). A promising specific capacitance of 851.4 F g^{-1} at 10 mV s^{-1} in 6 M KOH was reported for the core@shell electrode. In contrast, Co@CNT-NC and MF-C are only capable of providing a capacitive capability of 594.3 and 171.4 F g^{-1}, respectively. It evidently implied that the combination of Co and Co$_3$O$_4$ could enhance the electrochemical performance due to the synergistic effect, as

compared to the individual components. Meanwhile, the special architecture of tubular fibers and nanospheres was beneficial to improve the conductivity. In addition, multiple oxidation states of Co metal cations could enhance the capacitive performance. Furthermore, a low R$_{ct}$ of 0.2 Ω (as illustrated in **Figure 11B**) was recorded and the capacitance retention of 93.6% was achieved after 10,000 charging and discharging cycles at 1 A g^{-1}, showing the favorable rapid charge and electrolyte transfer processes resulting from the unique structure.

The electrochemical performance of some CNTs applied as SC electrode materials studied in the literatures is outlined in **Table 3**. Overall, CNT as 1D carbonaceous nanomaterials have attracted great research attention for electrochemical ESSs in recent years, mainly due to the excellent physiochemical strength and great electrical conductivity characteristics. To further enhance the capacitive performance, pseudocapacitive active materials (like TMOs, conductive polymers) are utilized to mix with CNTs for enhancing the capacitive performance. Meanwhile, it is a possible route to improve the specific capacitance by a combination of high porous carbons and CNTs. It is reasonable as the inlay of CNTs in highly porous carbons is beneficial to construct porous architectures with better conductivity and stability, which could be helpful to enhance electrochemical performance. Furthermore, heteroatom doping is another efficient approach to achieve high electrode performance.

CONCLUSION AND FUTURE PERSPECTIVES

In summary, this review presents an overview of the development of high-performance MOF materials with micro- and mesoporous structures for the application of electrochemical ESSs, particularly for SCs in the recent decade. In addition, the application of the pristine MOFs materials and their derivatives, such as carbon materials derived from MOFs, have been presented. Even though it is obvious that MOF-based materials exhibit many positive aspects, including large surface

TABLE 3 | The electrochemical performance of carbon nanotube (CNT) nanocomposites as electrodes for SCs.

Samples	Capacitance (F g^{-1}) at scan rate/Current density	Electrolyte	Potential window (V)	References electrode	Capacitance retention (%)/Cycle number	References
CNTs/AC	180 at 1 mV s^{-1}	1 M LiPF$_6$	2.5	—	90/5,000	Lei and Lekakou, (2013)
CNTs-T	3,199 at 5 mV s^{-1} 849 at 50 mV s^{-1}	0.075 M HQ + 1 M H$_2$SO$_4$	1	SCE	70/350	Wang et al. (2014)
ZFO-CNT	92.2 at 0.35 A g^{-1} 62.18 at 1.77 A g^{-1}	PVA-LiCl	1	—	70/2,000	Raut et al. (2018)
Co-Co$_3$O$_4$ @CNT-NC	823.4 at 1 A g^{-1} 653.7 at 15 A g^{-1}	6 M KOH	1.6	Ag/AgCl	93.6/10,000	Zou et al. (2018)
ECNT-PPy	214.99 at 0.22 A cm^{-1} 161.67 at 40 A cm^{-1}	SDBS + MgCl$_2$	1.9	SCE	89/10,000	Chang et al. (2018)
BCNT-CNF	207 at 1 A g^{-1} 139 at 10 A g^{-1}	1 M H$_2$SO$_4$	1	—	95.6/5,000	Zhou et al. (2019c)
NOPC/CNT-20	293.1 at 1 A g^{-1} 207 at 30 A g^{-1}	6 M KOH	1	Hg/HgO	99/10,000	Zhou et al. (2019b)
PANI/MWCNT	612.5 at 0.5 A g^{-1}	1 M H$_2$SO$_4$	0.8	SCE	81.5/5,000	Liu et al. (2018c)
Co-Ni-S/CNTs	540.6 C g^{-1} at 1 A g^{-1}	6 M KOH	1.6	Hg/HgO	83/10,000	Ma et al. (2021b)
CoZnNiS@ CNTs/rGO	1349.2 at 1 A g^{-1}	6 M KOH	1.7	Hg/HgO	90.6/10,000	Liu et al. (2021b)
N-CNT@CF	155 at 0.5 A g^{-1}	6 M KOH	1	—	93/10,000	Mofokeng et al. (2020)

areas, high porosity, and tunable sizes and structures, the application of MOFs in SC still faces a lot of challenges. For instance, most of the pristine MOFs are found to possess low conductivity and inferior cycling stability.

The performance of pristine MOFs and their derivatives (NPC) as electrode materials was discussed in detail. In general, majority of the pristine MOF materials possessed low conductivity, poor specific capacitance in aqueous-based electrolyte, and low operating voltage windows. Nonetheless, when TMOs and carbon derived from the MOF precursor are assembled into electrodes for HCs, significant enhancement in both electrochemical capacitance and cyclic stability are observed.

As illustrated by many previous studies, MOF materials with mesoporous (2–50 nm) structures displayed favorable performance in both specific capacitance and cyclic stability owing to the enhanced ionic transport and high accessible areas of the electroactive sites. It offers a promising route on the novel design of MOFs architectures for SCs, while most of the studies concentrate on low-valence-based MOFs; thus, it is necessary to explore the pristine MOFs with high-valence coordination such as Zr^{4+} and Cr^{3+} for SCs. As for nanocomposites derived from MOFs, an "all in one" strategy is an efficient approach to cope with low working voltage window and inferior performance issues. Most importantly, cyclic stability has become a main challenge for practical applications of MOF materials. Doping or co-doping of heteroatoms in MOF-derived NPC with excellent porosity is beneficial to facilitate the specific capacity and cyclic stability due to the synergistic effect.

Lastly, CNTs exhibit favorable features for ESSs, such as hollow structures formed by rolling single or multiple layers of graphene sheets, high mechanical strength, and excellent electrical conductivity. Furthermore, the integration of TMOs

and conducting polymers with CNTs are found able to enhance the electrochemical performance tremendously, and it is hence able to exert the superiorities simultaneously. Therefore, composite materials with high performance and low cost can be synthesized for mass production. This also offers a promising alternative route for future application of CNTs in electrochemical storage development.

Though MOF materials exhibit numerous advantages and show tremendous potential in ESSs, there are still some persistent challenges that need to be tackled comprehensively. Therefore, in the future study, more investigations on MOF-based SC electrode materials should be explored to construct ideal energy storage devices. Firstly, the conductive mechanisms in MOF materials should be widely explored, particularly for high-dimensional MOFs (e.g., 3D). Meanwhile, the electrical conductivity of pristine MOFs can be enhanced by incorporating highly conductive nanocomposites due to synergistic effects. Secondly, most MOF nanocomposites cannot possess the properties of high energy density and power density simultaneously; it is hence crucial for researchers to systematically explore advanced characterization tools and electrochemical mechanisms. Additionally, studies on the electrochemical performance of MOFs with multi-metal ions and multi-organic ligands are still rare, and great efforts should be made on this aspect. Lastly, electrolytes have a significant role to play in the electrochemical performance. The electrochemical performances of most MOF nanomaterials are studied in aqueous and organic-based electrolytes and ionic electrolytes with distinctive electrochemical stability, and wide operating potential windows might able to offer

realization on the development of a safe, durable, and sustainable SC system.

AUTHOR CONTRIBUTIONS

SZ and PK have made substantial contribution to the conceptual design of the manuscript; SZ drafted the manuscript preparation, while PK, SL, CF, CH, WC, and CC reviewed the manuscript critically and contributed important intellectual content to the article. Meanwhile, PK serves as the corresponding author on behalf of the authorship. All authors revised and approved the submission of final manuscript.

FUNDING

REFERENCES

Allendorf, M. D., Foster, M. E., Léonard, F., Stavila, V., Feng, P. L., Doty, F. P., et al. (2015). Guest-Induced Emergent Properties in Metal-Organic Frameworks. *J. Phys. Chem. Lett.* 6, 1182–1195. doi:10.1021/jz5026883

Bao, W., Mondal, A. K., Xu, J., Wang, C., Su, D., and Wang, G. (2016). 3D Hybrid-Porous Carbon Derived from Carbonization of Metal Organic Frameworks for High Performance Supercapacitors. *J. Power Sourc.* 325, 286–291. doi:10.1016/j.jpowsour.2016.06.037

Bonaccorso, F., Colombo, L., Yu, G., Stoller, M., Tozzini, V., Ferrari, A. C., et al. (2015). Graphene, Related Two-Dimensional Crystals, and Hybrid Systems for Energy Conversion and Storage. *Science.* 347, 1246501. doi:10.1126/science.1246501

Boota, M., and Gogotsi, Y. (2019). MXene-Conducting Polymer Asymmetric Pseudocapacitors. *Adv. Energ. Mater.* 9, 1802917. doi:10.1002/aenm.201802917

Cai, J., Song, Y., Chen, X., Sun, Z., Yi, Y., Sun, J., et al. (2020). MOF-Derived Conductive Carbon Nitrides for Separator-Modified Li-S Batteries and Flexible Supercapacitors. *J. Mater. Chem. A.* 8, 1757–1766. doi:10.1039/c9ta11958b

Campagnol, N., Romero-Vara, R., Deleu, W., Stappers, L., Binnemans, K., De Vos, D. E., et al. (2014). A Hybrid Supercapacitor Based on Porous Carbon and the Metal-Organic Framework MIL-100(Fe). *ChemElectroChem.* 1, 1182–1188. doi:10.1002/celc.201402022

Cao, C., Zhou, Y., Ubnoske, S., Zang, J., Cao, Y., Henry, P., et al. (2019a). Carbon Nanotubes: Highly Stretchable Supercapacitors *via* Crumpled Vertically Aligned Carbon Nanotube Forests (Adv. Energy Mater. 22/2019). *Adv. Energ. Mater.Advanced Energ. Mater.* 9, 1970082. doi:10.1002/aenm.201970082

Cao, C., Zhou, Y., Ubnoske, S., Zang, J., Cao, Y., Henry, P., et al. (2019b). Highly Stretchable Supercapacitors *via* Crumpled Vertically Aligned Carbon Nanotube Forests. *Adv. Energ. Mater.* 9, 1900618. doi:10.1002/aenm.201900618

Cao, X., Tan, C., Sindoro, M., and Zhang, H. (2017). Hybrid Micro-/Nano-Structures Derived From Metal-Organic Frameworks: Preparation and Applications in Energy Storage and Conversion. *Chem. Soc. Rev.* 46, 2660–2677. doi:10.1039/c6cs00426a

Cavka, J. H., Jakobsen, S., Olsbye, U., Guillou, N., Lamberti, C., Bordiga, S., et al. (2008). A New Zirconium Inorganic Building Brick Forming Metal Organic Frameworks With Exceptional Stability. *J. Am. Chem. Soc.* 130, 13850–13851. doi:10.1021/ja8057953

Chang, T.-H., Young, C., Lee, M.-H., Salunkhe, R. R., Alshehri, S. M., Ahamad, T., et al. (2017). Synthesis of MOF-525 Derived Nanoporous Carbons With Different Particle Sizes for Supercapacitor Application. *Chem. Asian J.* 12, 2857–2862. doi:10.1002/asia.201701082

Chang, Z.-H., Feng, D.-Y., Huang, Z.-H., and Liu, X.-X. (2018). Electrochemical Deposition of Highly Loaded Polypyrrole on Individual Carbon Nanotubes in Carbon Nanotube Film for Supercapacitor. *Chem. Eng. J.* 337, 552–559. doi:10.1016/j.cej.2017.12.095

Chen, Y., Wu, H., Lv, D., Yang, W., Qiao, Z., Li, Z., et al. (2018). An Ultramicroporous Nickel-Based Metal-Organic Framework for Adsorption Separation of CO2 Over N2 or CH4. *Energy Fuels.* 32, 8676–8682. doi:10.1021/acs.energyfuels.8b02287

Cheng, C., Xu, J., Gao, W., Jiang, S., and Guo, R. (2019). Preparation of Flexible Supercapacitor With RGO/Ni-MOF Film on Ni-Coated Polyester Fabric. *Electrochimica Acta.* 318, 23–31. doi:10.1016/j.electacta.2019.06.055

Chocarro-Ruiz, B., Pérez-Carvajal, J., Avci, C., Calvo-Lozano, O., Alonso, M. I., Maspoch, D., et al. (2018). A CO2Optical Sensor Based on Self-Assembled Metal-Organic Framework Nanoparticles. *J. Mater. Chem. A.* 6, 13171–13177. doi:10.1039/c8ta02767f

Choi, K. M., Jeong, H. M., Park, J. H., Zhang, Y. B., Kang, J. K., and Yaghi, O. M. (2014). *Supercapacitors of Nanocrystalline Metal Organic Frameworks*. Washington, DC: American Chemical Society.

Clough, A. J., Skelton, J. M., Downes, C. A., De La Rosa, A. A., Yoo, J. W., Walsh, A., et al. (2017). Metallic Conductivity in a Two-Dimensional Cobalt Dithiolene Metal-Organic Framework. *J. Am. Chem. Soc.* 139, 10863–10867. doi:10.1021/jacs.7b05742

Costentin, C., Porter, T. R., and Savéant, J.-M. (2017). How Do Pseudocapacitors Store Energy? Theoretical Analysis and Experimental Illustration. *ACS Appl. Mater. Inter.* 9, 8649–8658. doi:10.1021/acsami.6b14100

Dai, S., Liu, Z., Zhao, B., Zeng, J., Hu, H., Zhang, Q., et al. (2018a). A High-Performance Supercapacitor Electrode Based on N-Doped Porous Graphene. *J. Power Sourc.* 387, 43–48. doi:10.1016/j.jpowsour.2018.03.055

Dai, S., Yuan, Y., Yu, J., Tang, J., Zhou, J., and Tang, W. (2018b). Metal-Organic Framework-Templated Synthesis of Sulfur-Doped Core-Sheath Nanoarrays and Nanoporous Carbon for Flexible All-Solid-State Asymmetric Supercapacitors. *Nanoscale.* 10, 15454–15461. doi:10.1039/c8nr03743d

Dalstein, O., Ceratti, D. R., Boissière, C., Grosso, D., Cattoni, A., and Faustini, M. (2016). Nanoimprinted, Submicrometric, MOF-Based 2D Photonic Structures: Toward Easy Selective Vapors Sensing by a Smartphone Camera. *Adv. Funct. Mater.* 26, 81–90. doi:10.1002/adfm.201503016

Denny, M. S., Jr., Parent, L. R., Patterson, J. P., Meena, S. K., Pham, H., Abellan, P., et al. (2018). Transmission Electron Microscopy Reveals Deposition of Metal Oxide Coatings Onto Metal-Organic Frameworks. *J. Am. Chem. Soc.* 140, 1348–1357. doi:10.1021/jacs.7b10453

Ding, M., Cai, X., and Jiang, H.-L. (2019). Improving MOF Stability: Approaches and Applications. *Chem. Sci.* 10, 10209–10230. doi:10.1039/c9sc03916c

Dou, J.-H., Sun, L., Ge, Y., Li, W., Hendon, C. H., Li, J., et al. (2017). Signature of Metallic Behavior in the Metal-Organic Frameworks M3(hexaiminobenzene)2 (M = Ni, Cu). *J. Am. Chem. Soc.* 139, 13608–13611. doi:10.1021/jacs.7b07234

Du, P., Dong, Y., Liu, C., Wei, W., Liu, D., and Liu, P. (2018). Fabrication of Hierarchical Porous Nickel Based Metal-Organic Framework (Ni-MOF) Constructed With Nanosheets as Novel Pseudo-Capacitive Material for Asymmetric Supercapacitor. *J. Colloid Interf. Sci.* 518, 57–68. doi:10.1016/j.jcis.2018.02.010

El-Kady, M. F., Ihns, M., Li, M., Hwang, J. Y., Mousavi, M. F., Chaney, L., et al. (2015). Engineering Three-Dimensional Hybrid Supercapacitors and Microsupercapacitors for High-Performance Integrated Energy Storage. *Proc. Natl. Acad. Sci. USA.* 112, 4233–4238. doi:10.1073/pnas.1420398112

Feng, C., Lv, C.-P., Zhao, H., Li, Z.-Q., Xie, W.-N., Sun, L. N., et al. (2020). Structural Elucidation and Supercapacitive Performance on a Mn(II)-Based MOF. *Cryst. Growth Des.* 20, 5682–5687. doi:10.1021/acs.cgd.9b01013

Furukawa, H., Cordova, K. E., O'Keeffe, M., and Yaghi, O. M. (2013). The Chemistry and Applications of Metal-Organic Frameworks. *Science.* 341, 1230444. doi:10.1126/science.1230444

Gao, M., Fu, J., Wang, M., Wang, K., Wang, S., Wang, Z., et al. (2018). A Self-Template and Self-Activation Co-Coupling green Strategy to Synthesize High Surface Area Ternary-Doped Hollow Carbon Microspheres for High

Performance Supercapacitors. *J. Colloid Interf. Sci.* 524, 165–176. doi:10.1016/j.jcis.2018.04.027

Gao, W., Chen, D., Quan, H., Zou, R., Wang, W., Luo, X., et al. (2017). Fabrication of Hierarchical Porous Metal-Organic Framework Electrode for Aqueous Asymmetric Supercapacitor. *ACS Sustainable Chem. Eng.* 5, 4144–4153. doi:10.1021/acssuschemeng.7b00112

Gautham Prasad, G., Nidheeshshetty, S. T., and Rakshitha and Bommegowda, B, B. K. (2019). *Supercapacitor Technology and its Applications: A Review.* Bristol: IOP Publishing.

Genesio, G., Maynadié, J., Carboni, M., and Meyer, D. (2018). Recent Status on MOF Thin Films on Transparent Conductive Oxides Substrates (ITO or FTO). *New J. Chem.* 42, 2351–2363. doi:10.1039/c7nj03171h

Gong, Y.-N., Ouyang, T., He, C.-T., and Lu, T.-B. (2016). Photoinduced Water Oxidation by an Organic Ligand Incorporated into the Framework of a Stable Metal-Organic Framework. *Chem. Sci.* 7, 1070–1075. doi:10.1039/c5sc02679b

Goswami, S., Ray, D., Otake, K.-i., Kung, C.-W., Garibay, S. J., Islamoglu, T., et al. (2018). A Porous, Electrically Conductive Hexa-Zirconium(iv) Metal-Organic Framework. *Chem. Sci.* 9, 4477–4482. doi:10.1039/c8sc00961a

He, D., Gao, Y., Yao, Y., Wu, L., Zhang, J., Huang, Z.-H., et al. (2020). Asymmetric Supercapacitors Based on Hierarchically Nanoporous Carbon and ZnCo2O4 From a Single Biometallic Metal-Organic Frameworks (Zn/Co-MOF). *Front. Chem.* 8, 719. doi:10.3389/fchem.2020.00719

He, H., Sun, Q., Gao, W., Perman, J. A., Sun, F., Zhu, G., et al. (2018). A Stable Metal-Organic Framework Featuring a Local Buffer Environment for Carbon Dioxide Fixation. *Angew. Chem. Int. Ed.* 57, 4657–4662. doi:10.1002/anie.201801122

Herren, B., Larson, P., Saha, M., and Liu, Y. (2019). Enhanced Electrical Conductivity of Carbon Nanotube-Based Elastomer Nanocomposites Prepared by Microwave Curing. *Polymers.* 11, 1212. doi:10.3390/polym11071212

Huang, C., Hao, C., Ye, Z., Zhou, S., Wang, X., Zhu, L., et al. (2019). *In Situ* Growth of ZIF-8-Derived Ternary ZnO/ZnCo2O4/NiO for High Performance Asymmetric Supercapacitors. *Nanoscale.* 11, 10114–10128. doi:10.1039/c9nr02230a

Huang, N., Kirk, D. W., Thorpe, S. J., Liang, C., Xu, L., Li, W., et al. (2015). Effect of Carbon Nanotube Loadings on Supercapacitor Characteristics. *Int. J. Energ. Res.* 39, 336–343. doi:10.1002/er.3246

Javanbakht, S., Pooresmaeil, M., and Namazi, H. (2019). Green One-Pot Synthesis of Carboxymethylcellulose/Zn-Based Metal-Organic Framework/Graphene Oxide Bio-Nanocomposite as a Nanocarrier for Drug Delivery System. *Carbohydr. Polym.* 208, 294–301. doi:10.1016/j.carbpol.2018.12.066

Jayananda, D., Kularatna, N., and Ross, D. a. S. (2018). "Design Approach for Supercapacitor Assisted LED Lighting (SCALED) Technique for DC-Microgrids," in 2018 IEEE International Conference on Industrial Electronics for Sustainable Energy Systems (IESES), 27–31. doi:10.1109/ieses.2018.8349845

Jayananda, D., Kularatna, N., and Steyn-Ross, D. A. (2020). Supercapacitor-Assisted LED (SCALED) Technique for Renewable Energy Systems: a Very Low Frequency Design Approach With Short-term DC-UPS Capability Eliminating Battery banks. *IET Renew. Power Generation.* 14, 1559–1570. doi:10.1049/iet-rpg.2019.1307

Jiang, H., Lee, P. S., and Li, C. (2013). 3D Carbon Based Nanostructures for Advanced Supercapacitors. *Energy Environ. Sci.* 6, 41–53. doi:10.1039/c2ee23284g

Jiang, Y., and Liu, J. (2019). Definitions of Pseudocapacitive Materials: A Brief Review. *Energy Environ. Mater.* 2, 30–37. doi:10.1002/eem2.12028

Jiang, Y., Li, J., Jiang, Z., Shi, M., Sheng, R., Liu, Z., et al. (2021). Large-Surface-Area Activated Carbon With High Density by Electrostatic Densification for Supercapacitor Electrodes. *Carbon* 175, 281–288. doi:10.1016/j.carbon.2021.01.016

Jin, L.-Q., Zheng, Y., Li, J.-H., and Liu, Y.-L. (2015). A Study of Novel Regenerative Braking System Based on Supercapacitor for Electric Vehicle Driven by In-Wheel Motors. *Adv. Mech. Eng.* 7, 168781401557376. doi:10.1177/1687814015573762

Kang, Z., Fan, L., and Sun, D. (2017). Recent Advances and Challenges of Metal-Organic Framework Membranes for Gas Separation. *J. Mater. Chem. A* 5, 10073–10091. doi:10.1039/c7ta01142c

Kannangara, Y. Y., Rathnayake, U. A., and Song, J.-K. (2019). Redox Active Multi-Layered Zn-pPDA MOFs as High-Performance Supercapacitor

Electrode Material. *Electrochimica acta.* 297, 145–154. doi:10.1016/j.electacta.2018.11.186

Kiani, M. A., Rahmanifar, M. S., El-Kady, M. F., Kaner, R. B., and Mousavi, M. F. (2015). Fabrication of High Power LiNi0.5Mn1.5O4 Battery Cathodes by Nanostructuring of Electrode Materials. *RSC Adv.* 5, 50433–50439. doi:10.1039/c5ra08170j

Kim, B. K., Sy, S., Yu, A., and Zhang, J. (2015). Electrochemical Supercapacitors for Energy Storage and Conversion. *Handbook Clean. Energ. Syst.* 5, 1–25. doi:10.1002/9781118991978.hces112

Kim, D. K., Bong, S., Jin, X., Seong, K.-d., Hwang, M., Kim, N. D., et al. (2019). Facile *In Situ* Synthesis of Multiple-Heteroatom-Doped Carbons Derived from Polyimide Precursors for Flexible All-Solid-State Supercapacitors. *ACS Appl. Mater. Inter.* 11, 1996–2005. doi:10.1021/acsami.8b15162

Kim, K. H., Oh, Y., and Islam, M. F. (2013). Mechanical and Thermal Management Characteristics of Ultrahigh Surface Area Single-Walled Carbon Nanotube Aerogels. *Adv. Funct. Mater.* 23, 377–383. doi:10.1002/adfm.201201055

Ko, M., Mendecki, L., and Mirica, K. A. (2018). Conductive Two-Dimensional Metal-Organic Frameworks as Multifunctional Materials. *Chem. Commun.* 54, 7873–7891. doi:10.1039/c8cc02871k

Kong, Y., Nanjundan, A. K., Liu, Y., Song, H., Huang, X., and Yu, C. (2019). Modulating Ion Diffusivity and Electrode Conductivity of Carbon Nanotube@Mesoporous Carbon Fibers for High Performance Aluminum-Selenium Batteries. *Small.* 15, e1904310. doi:10.1002/smll.201904310

Lei, C., and Lekakou, C. (2013). Activated Carbon-Carbon Nanotube Nanocomposite Coatings for Supercapacitor Applications. *Surf. Coat. Technology.* 232, 326–330. doi:10.1016/j.surfcoat.2013.05.027

Li, B., Wen, H.-M., Zhou, W., and Chen, B. (2014). Porous Metal-Organic Frameworks for Gas Storage and Separation: What, How, and Why? *J. Phys. Chem. Lett.* 5, 3468–3479. doi:10.1021/jz501586e

Li, J., Qiu, S., Liu, B., Chen, H., Xiao, D., and Li, H. (2021). Strong Interaction Between Polyaniline and Carbon Fibers for Flexible Supercapacitor Electrode Materials. *J. Power Sourc.* 483. doi:10.1016/j.jpowsour.2020.229219

Li, J., and Xu, Z. (2019). Few-walled Carbon Nanotube-Enhanced Activated Carbon Supercapacitor Performance in Organic Electrolyte at 4 V. *RSC Adv.* 9, 18863–18867. doi:10.1039/c9ra02641j

Li, N., Xu, J., Feng, R., Hu, T.-L., and Bu, X.-H. (2016). Governing Metal-Organic Frameworks Towards High Stability. *Chem. Commun.* 52, 8501–8513. doi:10.1039/c6cc02931k

Lin, S., Usov, P. M., and Morris, A. J. (2018). The Role of Redox Hopping in Metal-Organic Framework Electrocatalysis. *Chem. Commun.* 54, 6965–6974. doi:10.1039/c8cc01664j

Liu, L., Yan, Y., Cai, Z., Lin, S., and Hu, X. (2018a). Growth-Oriented Fe-Based MOFs Synergized With Graphene Aerogels for High-Performance Supercapacitors. *Adv. Mater. Inter.* 5, 1701548. doi:10.1002/admi.201701548

Liu, M., Zhao, F., Zhu, D., Duan, H., Lv, Y., Li, L., et al. (2018b). Ultramicroporous Carbon Nanoparticles Derived from Metal-Organic Framework Nanoparticles for High-Performance Supercapacitors. *Mater. Chem. Phys.* 211, 234–241. doi:10.1016/j.matchemphys.2018.02.030

Liu, Q., Bai, Z., Fan, J., Sun, Z., Mi, H., Zhang, Q., et al. (2018c). A Hydrogel-Mediated Scalable Strategy Toward Core-Shell Polyaniline/Poly(Acrylic Acid)-Modified Carbon Nanotube Hybrids as Efficient Electrodes for Supercapacitor Applications. *Appl. Surf. Sci.* 436, 189–197. doi:10.1016/j.apsusc.2017.11.209

Liu, Q., Liu, X., Shi, C., Zhang, Y., Feng, X., Cheng, M.-L., et al. (2015a). A Copper-Based Layered Coordination Polymer: Synthesis, Magnetic Properties and Electrochemical Performance in Supercapacitors. *Dalton Trans.* 44, 19175–19184. doi:10.1039/c5dt02918j

Liu, X., Demir, N. K., Wu, Z., and Li, K. (2015b). Highly Water-Stable Zirconium Metal-Organic Framework UiO-66 Membranes Supported on Alumina Hollow Fibers for Desalination. *J. Am. Chem. Soc.* 137, 6999–7002. doi:10.1021/jacs.5b02276

Liu, W., Zhu, F., Ge, B., Sun, L., Liu, Y., and Shi, W. (2021a). MOF Derived ZnO/C@(Ni,Co)Se2 Core–Shell Nanostructure on Carbon Cloth for High-Performance Supercapacitors. *Chem. Eng. J.* 427, 130788. doi:10.1016/j.cej.2021.131503

Liu, Y., Huo, Y., Wang, X., Yu, S., Ai, Y., Chen, Z., et al. (2021b). Impact of Metal Ions and Organic Ligands on Uranium Removal Properties by Zeolitic Imidazolate Framework Materials. *J. Clean. Prod.* 278. doi:10.1016/j.jclepro.2020.123216

Liu, Y., Xin, N., Yang, Q., and Shi, W. (2021c). 3D CNTs/graphene Network Conductive Substrate Supported MOFs-Derived CoZnNiS Nanosheet Arrays for Ultra-high Volumetric/gravimetric Energy Density Hybrid Supercapacitor. *J. Colloid Interf. Sci.* 583, 288–298. doi:10.1016/j.jcis.2020.08.128

Liu, Y., An, Z., Wu, M., Yuan, A., Zhao, H., Zhang, J., et al. (2020). Peony Pollen Derived Nitrogen-Doped Activated Carbon for Supercapacitor Application. *Chin. Chem. Lett.* 31, 1644–1647. doi:10.1016/j.cclet.2019.08.005

Lv, X.-L., Yuan, S., Xie, L.-H., Darke, H. F., Chen, Y., He, T., et al. (2019). Ligand Rigidification for Enhancing the Stability of Metal-Organic Frameworks. *J. Am. Chem. Soc.* 141, 10283–10293. doi:10.1021/jacs.9b02947

Ma, W., Xie, L., Dai, L., Sun, G., Chen, J., Su, F., et al. (2018). Influence of Phosphorus Doping on Surface Chemistry and Capacitive Behaviors of Porous Carbon Electrode. *Electrochimica Acta.* 266, 420–430. doi:10.1016/j.electacta.2018.02.031

Ma, Y., Gao, G., Su, H., Rong, H., Lai, L., and Liu, Q. (2021a). A Cu4 Cluster-Based MOF as a Supercapacitor Electrode Material With Ultrahigh Capacitance. *Ionics.* 27, 1699–1707. doi:10.1007/s11581-021-03954-w

Ma, Z., Zheng, R., Liu, Y., Ying, Y., and Shi, W. (2021b). Carbon Nanotubes Interpenetrating MOFs-Derived Co-ni-S Composite Spheres With Interconnected Architecture for High Performance Hybrid Supercapacitor. *J. Colloid Interf. Sci.* 602, 627–635. doi:10.1016/j.jcis.2021.06.027

Manjakkal, L., Núñez, C. G., Dang, W., and Dahiya, R. (2018). Flexible Self-Charging Supercapacitor Based on Graphene-Ag-3d Graphene Foam Electrodes. *Nano Energy.* 51, 604–612. doi:10.1016/j.nanoen.2018.06.072

Meng, Z., Aykanat, A., and Mirica, K. A. (2019). Welding Metallophthalocyanines Into Bimetallic Molecular Meshes for Ultrasensitive, Low-Power Chemiresistive Detection of Gases. *J. Am. Chem. Soc.* 141, 2046–2053. doi:10.1021/jacs.8b11257

Mofokeng, T. P., Tetana, Z. N., and Ozoemena, K. I. (2020). Defective 3D Nitrogen-Doped Carbon Nanotube-Carbon Fibre Networks for High-Performance Supercapacitor: Transformative Role of Nitrogen-Doping from Surface-Confined to Diffusive Kinetics. *Carbon.* 169, 312–326. doi:10.1016/j.carbon.2020.07.049

Nadar, S. S., and Rathod, V. K. (2018). Magnetic-metal Organic Framework (Magnetic-MOF): A Novel Platform for Enzyme Immobilization and Nanozyme Applications. *Int. J. Biol. Macromolecules.* 120, 2293–2302. doi:10.1016/j.ijbiomac.2018.08.126

Nguyen, D. K., Schepisi, I. M., and Amir, F. Z. (2019). Extraordinary Cycling Stability of Ni$_3$(HITP)$_2$ Supercapacitors Fabricated by Electrophoretic Deposition: Cycling at 100,000 Cycles. *Chem. Eng. J.* 378. doi:10.1016/j.cej.2019.122150

Ni, G., Qin, F., Guo, Z., Wang, J., and Shen, W. (2020). Nitrogen-doped Asphaltene-Based Porous Carbon Fibers as Supercapacitor Electrode Material With High Specific Capacitance. *Electrochimica acta.* 330, 135270. doi:10.1016/j.electacta.2019.135270

Olajire, A. A. (2018). Synthesis Chemistry of Metal-Organic Frameworks for CO 2 Capture and Conversion for Sustainable Energy Future. *Renew. Sustainable Energ. Rev.* 92, 570–607. doi:10.1016/j.rser.2018.04.073

Partridge, J., and Abouelamaimen, D. I. (2019). The Role of Supercapacitors in Regenerative Braking Systems. *Energies.* 12, 2683. doi:10.3390/en12142683

Pavaskar, G., Ramakrishnasubramanian, K., Kandagal, V. S., and Kumar, P. (2018). Modeling Electric Double-Layer Capacitors Using Charge Variation Methodology in Gibbs Ensemble. *Front. Energ. Res.* 5, 36. doi:10.3389/fenrg.2017.00036

Qin, R., Qian, Q., Liu, Y., Ou, A., Li, Y., Liu, X., et al. (2019a). Preparing Nitrogen-Doped Multiwalled Carbon Nanotubes With Regionally Controllable Heterojunction Structure by Nondestructive Postdoping With the Assistance of Heating Fluorination. *J. Phys. Chem. C.* 123, 16439–16448. doi:10.1021/acs.jpcc.9b03884

Qin, T., Chen, H., Zhang, Y., Chen, X., Liu, L., Yan, D., et al. (2019b). Modulating Surface Chemistry of Heteroatom-Rich Micropore Carbon Cloth Electrode for Aqueous 2.1 V High-Voltage Window All-Carbon Supercapacitor. *J. Power Sourc.* 431, 232–238. doi:10.1016/j.jpowsour.2019.05.004

Rakhi, R. B., Chen, W., Cha, D., and Alshareef, H. N. (2012). Nanostructured Ternary Electrodes for Energy-Storage Applications. *Adv. Energ. Mater.* 2, 381–389. doi:10.1002/aenm.201100609

Ramachandran, R., Zhao, C., Luo, D., Wang, K., and Wang, F. (2018). Morphology-Dependent Electrochemical Properties of Cobalt-Based Metal Organic Frameworks for Supercapacitor Electrode Materials. *Electrochimica Acta.* 267, 170–180. doi:10.1016/j.electacta.2018.02.074

Raut, S. S., Sankapal, B. R., Hossain, M. S. A., Pradhan, S., Salunkhe, R. R., and Yamauchi, Y. (2018). Zinc Ferrite Anchored Multiwalled Carbon Nanotubes for High-Performance Supercapacitor Applications. *Eur. J. Inorg. Chem.* 2018, 137–142. doi:10.1002/ejic.201700836

Ray, D., Goswami, S., Duan, J., Hupp, J. T., Cramer, C. J., and Gagliardi, L. (2021). Tuning the Conductivity of Hexa-Zirconium(IV) Metal-Organic Frameworks by Encapsulating Heterofullerenes. *Chem. Mater.* 33, 1182–1189. doi:10.1021/acs.chemmater.0c03855

Salunkhe, R. R., Kamachi, Y., Torad, N. L., Hwang, S. M., Sun, Z., Dou, S. X., et al. (2014). Fabrication of Symmetric Supercapacitors Based on MOF-Derived Nanoporous Carbons. *J. Mater. Chem. A.* 2, 19848–19854. doi:10.1039/c4ta04277h

Salunkhe, R. R., Kaneti, Y. V., and Yamauchi, Y. (2017). Metal-Organic Framework-Derived Nanoporous Metal Oxides Toward Supercapacitor Applications: Progress and Prospects. *ACS Nano.* 11, 5293–5308. doi:10.1021/acsnano.7b02796

Schoenecker, P. M., Carson, C. G., Jasuja, H., Flemming, C. J. J., and Walton, K. S. (2012). Effect of Water Adsorption on Retention of Structure and Surface Area of Metal-Organic Frameworks. *Ind. Eng. Chem. Res.* 51, 6513–6519. doi:10.1021/ie202325p

Sengupta, A., Datta, S., Su, C., Herng, T. S., Ding, J., Vittal, J. J., et al. (2016). Tunable Electrical Conductivity and Magnetic Property of the Two Dimensional Metal Organic Framework [Cu(TPyP)Cu2(O2CCH3)4]. *ACS Appl. Mater. Inter.* 8, 16154–16159. doi:10.1021/acsami.6b03073

Senkovska, I., and Kaskel, S. (2014). Ultrahigh Porosity in Mesoporous MOFs: Promises and Limitations. *Chem. Commun. (Camb).* 50, 7089–7098. doi:10.1039/c4cc00524d

Sezginel, K. B., Asinger, P. A., Babaei, H., and Wilmer, C. E. (2018). Thermal Transport in Interpenetrated Metal-Organic Frameworks. *Chem. Mater.* 30, 2281–2286. doi:10.1021/acs.chemmater.7b05015

Shi, M., Huang, R., Qi, W., Su, R., and He, Z. (2020). Synthesis of Superhydrophobic and High Stable Zr-MOFs for Oil-Water Separation. *Colloids Surf. A: Physicochemical Eng. Aspects.* 602, 125102. doi:10.1016/j.colsurfa.2020.125102

Shih, Y.-H., Kuo, Y.-C., Lirio, S., Wang, K.-Y., Lin, C.-H., and Huang, H.-Y. (2017). A Simple Approach to Enhance the Water Stability of a Metal-Organic Framework. *Chem. Eur. J.* 23, 42–46. doi:10.1002/chem.201603647

Shinde, P. A., Seo, Y., Lee, S., Kim, H., Pham, Q. N., Won, Y., et al. (2020). Layered Manganese Metal-Organic Framework With High Specific and Areal Capacitance for Hybrid Supercapacitors. *Chem. Eng. J.* 387, 122982. doi:10.1016/j.cej.2019.122982

Stassen, I., Styles, M., Van Assche, T., Campagnol, N., Fransaer, J., Denayer, J., et al. (2015). Electrochemical Film Deposition of the Zirconium Metal-Organic Framework UiO-66 and Application in a Miniaturized Sorbent Trap. *Chem. Mater.* 27, 1801–1807. doi:10.1021/cm504806p

Sun, L., Hendon, C. H., Minier, M. A., Walsh, A., and Dincă, M. (2015). Million-Fold Electrical Conductivity Enhancement in Fe2(DEBDC) Versus Mn2(DEBDC) (E = S, O). *J. Am. Chem. Soc.* 137, 6164–6167. doi:10.1021/jacs.5b02897

Sun, L., Hendon, C. H., Park, S. S., Tulchinsky, Y., Wan, R., Wang, F., et al. (2017). Is Iron Unique in Promoting Electrical Conductivity in MOFs? *Chem. Sci.* 8, 4450–4457. doi:10.1039/c7sc00647k

Sun, L., Miyakai, T., Seki, S., and Dincă, M. (2013). Mn2(2,5-disulfhydrylbenzene-1,4-dicarboxylate): A Microporous Metal-Organic Framework With Infinite (−Mn−S−)∞ Chains and High Intrinsic Charge Mobility. *J. Am. Chem. Soc.* 135, 8185–8188. doi:10.1021/ja4037516

Sundriyal, S., Kaur, H., Bhardwaj, S. K., Mishra, S., Kim, K.-H., and Deep, A. (2018). Metal-Organic Frameworks and Their Composites as Efficient Electrodes for Supercapacitor Applications. *Coord. Chem. Rev.* 369, 15–38. doi:10.1016/j.ccr.2018.04.018

Sundriyal, S., Mishra, S., and Deep, A. (2019). Study of Manganese-1,4-Benzenedicarboxylate Metal Organic Framework Electrodes Based Solid State Symmetrical Supercapacitor. *Energ. Proced.* 158, 5817–5824. doi:10.1016/j.egypro.2019.01.546

Sundriyala, S., Mishra, S., and Deep, A. (2019). *Study of Manganese-1,4-Benzenedicarboxylate Metal Organic Framework Electrodes Based Solid State Symmetrical Supercapacitor*. Amsterdam, Elsevier: Energy Procedia.

Tan, Y., Zhang, W., Gao, Y., Wu, J., and Tang, B. (2015). Facile Synthesis and Supercapacitive Properties of Zr-Metal Organic Frameworks (UiO-66). *RSC Adv.* 5, 17601–17605. doi:10.1039/c4ra11896k

Tang, Z., Zhang, G., Zhang, H., Wang, L., Shi, H., Wei, D., et al. (2018). MOF-Derived N-Doped Carbon Bubbles on Carbon Tube Arrays for Flexible High-Rate Supercapacitors. *Energ. Storage Mater.* 10, 75–84. doi:10.1016/j.ensm.2017.08.009

Wang, C., Liu, C., Li, J., Sun, X., Shen, J., Han, W., et al. (2017a). Electrospun Metal-Organic Framework Derived Hierarchical Carbon Nanofibers with High Performance for Supercapacitors. *Chem. Commun.* 53, 1751–1754. doi:10.1039/c6cc09832k

Wang, X., Liu, X., Rong, H., Song, Y., Wen, H., and Liu, Q. (2017b). Layered Manganese-Based Metal-Organic Framework as a High Capacity Electrode Material for Supercapacitors. *RSC Adv.* 7, 29611–29617. doi:10.1039/c7ra04374k

Wang, X., Zheng, Y., Yuan, J., Shen, J., Niu, L., and Wang, A.-j. (2017c). Controllable Synthesis of Caterpillar-Like Molybdenum Sulfide @Carbon Nanotube Hybrids with Core Shell Structure for Hydrogen Evolution. *Electrochimica acta.* 235, 422–428. doi:10.1016/j.electacta.2017.02.093

Wang, F., Ma, J., Zhou, K., and Li, X. (2020a). MoS2/Corncob-Derived Activated Carbon for Supercapacitor Application. *Mater. Chem. Phys.* 244, 122215. doi:10.1016/j.matchemphys.2019.122215

Wang, K.-B., Xun, Q., and Zhang, Q. (2020b). Recent Progress in Metal-Organic Frameworks as Active Materials for Supercapacitors. *EnergyChem.* 2, 100025. doi:10.1016/j.enchem.2019.100025

Wang, K., Li, Q., Ren, Z., Li, C., Chu, Y., Wang, Z., et al. (2020c). 2D Metal-Organic Frameworks (MOFs) for High-Performance BatCap Hybrid Devices. *Small.* 16, 2001987. doi:10.1002/smll.202001987

Wang, Y., Liu, R., Tian, Y., Sun, Z., Huang, Z., Wu, X., et al. (2020d). Heteroatoms-Doped Hierarchical Porous Carbon Derived From Chitin for Flexible All-Solid-State Symmetric Supercapacitors. *Chem. Eng. J.* 384, 123263. doi:10.1016/j.cej.2019.123263

Wang, Y., Xie, X., Zhang, B., Luo, J., Wang, S., Nie, S., et al. (2020e). A New Cd-Based Metal Organic Framework Derived Nitrogen Doped Nano-Porous Carbon for High Supercapacitor Performance. *Polyhedron.* 189, 114726. doi:10.1016/j.poly.2020.114726

Wang, G., Liang, R., Liu, L., and Zhong, B. (2014). Improving the Specific Capacitance of Carbon Nanotubes-Based Supercapacitors by Combining Introducing Functional Groups on Carbon Nanotubes With Using Redox-Active Electrolyte. *Electrochimica Acta.* 115, 183–188. doi:10.1016/j.electacta.2013.10.165

Wang, Q., Shao, L., Ma, Z., Xu, J., Li, Y., and Wang, C. (2018). Hierarchical Porous PANI/MIL-101 Nanocomposites Based Solid-State Flexible Supercapacitor. *Electrochimica Acta.* 281, 582–593. doi:10.1016/j.electacta.2018.06.002

Wang, Y., Song, Y., and Xia, Y. (2016). Electrochemical Capacitors: Mechanism, Materials, Systems, Characterization and Applications. *Chem. Soc. Rev.* 45, 5925–5950. doi:10.1039/c5cs00580a

Wang, Z., Huang, J., Guo, Z., Dong, X., Liu, Y., Wang, Y., et al. (2019). A Metal-Organic Framework Host for Highly Reversible Dendrite-Free Zinc Metal Anodes. *Joule.* 3, 1289–1300. doi:10.1016/j.joule.2019.02.012

Wechsler, S. C., and Amir, F. Z. (2020). Superior Electrochemical Performance of Pristine Nickel Hexaaminobenzene MOF Supercapacitors Fabricated by Electrophoretic Deposition. *ChemSusChem.* 13, 1491–1495. doi:10.1002/cssc.201902691

Wu, S. C., Chang, P. H., Chou, S. H., Huang, C. Y., Liu, T. C., and Peng, C. H. (2020). Waffle-Like Carbons Combined With Enriched Mesopores and Highly Heteroatom-Doped Derived from Sandwiched MOF/LDH/MOF for High-Rate Supercapacitor. *Nanomaterials (Basel).* 10. doi:10.3390/nano10122388

Xia, W., Mahmood, A., Zou, R., and Xu, Q. (2015). Metal-organic Frameworks and Their Derived Nanostructures for Electrochemical Energy Storage and Conversion. *Energ. Environ. Sci.* 8, 1837–1866. doi:10.1039/c5ee00762c

Xia, W., Qu, C., Liang, Z., Zhao, B., Dai, S., Qiu, B., et al. (2017). High-Performance Energy Storage and Conversion Materials Derived from a Single Metal-Organic Framework/Graphene Aerogel Composite. *Nano Lett.* 17, 2788–2795. doi:10.1021/acs.nanolett.6b05004

Xiao, L., Lin, L., and Liu, Y. (2011). Discussions on the Architecture and Operation Mode of Future Power Grids. *Energies.* 4, 1025–1035. doi:10.3390/en4071025

Xie, L. S., Skorupskii, G., and Dincă, M. (2020). Electrically Conductive Metal-Organic Frameworks. *Chem. Rev.* 120, 8536–8580. doi:10.1021/acs.chemrev.9b00766

Xiong, X., Zhou, L., Cao, W., Liang, J., Wang, Y., Hu, S., et al. (2017). Metal-Organic Frameworks Based on Halogen-Bridged Dinuclear-Cu-Nodes as Promising Materials for High Performance Supercapacitor Electrodes. *CrystEngComm.* 19, 7177–7184. doi:10.1039/c7ce01840a

Xu, J., Yang, Y., Wang, Y., Cao, J., and Chen, Z. (2019). Enhanced Electrochemical Properties of Manganese-Based Metal Organic Framework Materials for Supercapacitors. *J. Appl. Electrochem.* 49, 1091–1102. doi:10.1007/s10800-019-01352-9

Xuan, W., Ramachandran, R., Zhao, C., and Wang, F. (2018). Influence of Synthesis Temperature on Cobalt Metal-Organic Framework (Co-MOF) Formation and its Electrochemical Performance Towards Supercapacitor Electrodes. *J. Solid State. Electrochem.* 22, 3873–3881. doi:10.1007/s10008-018-4096-7

Yan, Y., Gu, P., Zheng, S., Zheng, M., Pang, H., and Xue, H. (2016). Facile Synthesis of an Accordion-Like Ni-MOF Superstructure for High-Performance Flexible Supercapacitors. *J. Mater. Chem. A.* 4, 19078–19085. doi:10.1039/c6ta08331e

Yang, C., Kaipa, U., Mather, Q. Z., Wang, X., Nesterov, V., Venero, A. F., et al. (2011). Fluorous Metal-Organic Frameworks with Superior Adsorption and Hydrophobic Properties Toward Oil Spill Cleanup and Hydrocarbon Storage. *J. Am. Chem. Soc.* 133, 18094–18097. doi:10.1021/ja208408n

Yang, C., Li, X., Yu, L., Liu, X., Yang, J., and Wei, M. (2020). A New Promising Ni-MOF Superstructure for High-Performance Supercapacitors. *Chem. Commun.* 56, 1803–1806. doi:10.1039/c9cc09302h

Yang, J., Ma, Z., Gao, W., and Wei, M. (2017). Layered Structural Co-Based MOF With Conductive Network Frames as a New Supercapacitor Electrode. *Chem. Eur. J.* 23, 631–636. doi:10.1002/chem.201604071

Yang, S. J., and Park, C. R. (2012). Preparation of Highly Moisture-Resistant Black-Colored Metal Organic Frameworks. *Adv. Mater.* 24, 4010–4013. doi:10.1002/adma.201200790

Yang, Y., Chen, L., Jiang, F., Wu, M., Pang, J., Wan, X., et al. (2019). A Water-Stable 3D Eu-MOF Based on a Metallacyclodimeric Secondary Building Unit for Sensitive Fluorescent Detection of Acetone Molecules. *CrystEngComm.* 21, 321–328. doi:10.1039/c8ce01875h

Yao, Y., Ma, C., Wang, J., Qiao, W., Ling, L., and Long, D. (2015). Rational Design of High-Surface-Area Carbon Nanotube/Microporous Carbon Core-Shell Nanocomposites for Supercapacitor Electrodes. *ACS Appl. Mater. Inter.* 7, 4817–4825. doi:10.1021/am5087374

Yi-Ju, L., Jin-Hui, Z., and Shao-Jun, G. (2019). Advanced Carbon Materials for Non-Aqueous Potassium Ion Battery Anodes. *Chinese Journal Structural Chemistry.* 38, 1993–1998. doi:10.14102/j.cnki.0254-5861.2011-2674

You, P. Y., and Kamarudin, S. K. (2017). Recent Progress of Carbonaceous Materials in Fuel Cell Applications: An Overview. *Chem. Eng. J.* 309, 489–502. doi:10.1016/j.cej.2016.10.051

Yue, D., Yang, J.-x., Sun, B., Shi, K., Zhu, H., and Li, X.-k. (2020). Preparation and Electrochemical Performance of the N-Doped Hollow Pitch-Based Activated Carbon Fibers as Supercapacitor Electrodes. *Carbon.* 167, 931. doi:10.1016/j.carbon.2020.04.052

Yue, M.-L., Yu, C.-Y., Duan, H.-H., Yang, B.-L., Meng, X.-X., and Li, Z.-X. (2018). Six Isomorphous Window-Beam MOFs: Explore the Effects of Metal Ions on MOF-Derived Carbon for Supercapacitors. *Chem. Eur. J.* 24, 16160–16169. doi:10.1002/chem.201803554

Zeng, L., Lou, X., Zhang, J., Wu, C., Liu, J., and Jia, C. (2019). Carbonaceous Mudstone and Lignin-Derived Activated Carbon and its Application for Supercapacitor Electrode. *Surf. Coat. Technology.* 357, 580–586. doi:10.1016/j.surfcoat.2018.10.041

Zheng, J., Tian, J., Wu, D., Gu, M., Xu, W., Wang, C., et al. (2014). Lewis Acid-Base Interactions between Polysulfides and Metal Organic Framework in Lithium Sulfur Batteries. *Nano Lett.* 14, 2345–2352. doi:10.1021/nl404721h

Zheng, S., Li, X., Yan, B., Hu, Q., Xu, Y., Xiao, X., et al. (2017). Transition-Metal (Fe, Co, Ni) Based Metal-Organic Frameworks for Electrochemical Energy Storage. *Adv. Energ. Mater.* 7, 1602733. doi:10.1002/aenm.201602733

Zhou, Q., Fan, T., Li, Y., Chen, D., Liu, S., and Li, X. (2019a). Hollow-Structure NiCo Hydroxide/Carbon Nanotube Composite for High-Performance

Supercapacitors. *J. Power Sourc.* 426, 111–115. doi:10.1016/j.jpowsour.2019.04.035

Zhou, Y., Song, Z., Hu, Q., Zheng, Q., Jiang, N., Xie, F., et al. (2019b). Hierarchical Nitrogen-Doped Porous Carbon/Carbon Nanotube Composites for High-Performance Supercapacitor. *Superlattices and Microstructures.* 130, 50–60. doi:10.1016/j.spmi.2019.04.013

Zhou, Y., Zhou, X., Ge, C., Zhou, W., Zhu, Y., and Xu, B. (2019c). Branched Carbon Nanotube/Carbon Nanofiber Composite for Supercapacitor Electrodes. *Mater. Lett.* 246, 174–177. doi:10.1016/j.matlet.2019.03.074

Zhu, G., Wen, H., Ma, M., Wang, W., Yang, L., Wang, L., et al. (2018). A Self-Supported Hierarchical Co-MOF as a Supercapacitor Electrode with Ultrahigh Areal Capacitance and Excellent Rate Performance. *Chem. Commun.* 54, 10499–10502. doi:10.1039/c8cc03669a

Zou, Y., Cai, C., Xiang, C., Huang, P., Chu, H., She, Z., et al. (2018). Simple Synthesis of Core-Shell Structure of Co-Co3O4 @ Carbon-Nanotube-Incorporated Nitrogen-Doped Carbon for High-Performance Supercapacitor. *Electrochimica Acta.* 261, 537–547. doi:10.1016/j.electacta.2017.12.184